Bystander memory-phenotype conventional CD4$^+$ T cells exacerbating autoimmune neuroinflammation

Min-Zi Cho[1,†], Hong-Gyun Lee[1,2,†], Jae-Won Yoon[1], Gil-Ran Kim[1], Ja-Hyun Koo[1,3], Reshma Taneja[4], Brian T. Edelson[5], You Jeong Lee[6], Je-Min Choi[1,7,8,*]

[1]Department of Life Science, College of Natural Sciences, Hanyang University, Seoul 04763, Republic of Korea.

[2]Ann Romney Center for Neurologic Diseases, Brigham and Women's Hospital, Harvard Medical School, Boston, MA 02115, USA.

[3]The Ragon Institute of Massachusetts General Hospital, Massachusetts Institute of Technology and Harvard University, Cambridge, MA 02139, USA.

[4]Department of Physiology and Healthy Longevity Translation Research Program, Yong Loo Lin School of Medicine, National University of Singapore, Singapore 117593.

[5]Department of Pathology and Immunology, Division of Laboratory and Genomic Medicine, Washington University School of Medicine, St. Louis, MO 63119, USA.

[6]Research Institute of Pharmaceutical Sciences, Seoul National University, Seoul, Republic of Korea.

[7]Research Institute for Natural Sciences, Hanyang University, Seoul 04763, Republic of Korea.

[8]Research Institute for Convergence of Basic Sciences, Hanyang University, Seoul 04763, Republic of Korea.

†These authors contributed equally to this work.

[*]Corresponding author. Email: jeminchoi@hanyang.ac.kr

Keywords: Memory-phenotype CD4$^+$ T cells, Bystander, EAE, Autoimmune neuroinflammation, CCR6, TCR independent, Bhlhe40

Abstract

Memory-phenotype (MP) $CD4^+$ T cells are a substantial population of conventional T cells that exist in steady-state mice, and their immunologic functions in autoimmune disease have not yet been studied. In this work, we unveil a unique phenotype of MP $CD4^+$ T cells by analyzing single-cell transcriptomics and T cell receptor (TCR) repertoires. We found that steady-state MP $CD4^+$ T cells exist regardless of germ and food-antigen which are composed of heterogenous effector subpopulations. Distinct subpopulations of MP $CD4^+$ T cells are specifically activated by IL-1 family cytokines and STAT activators, revealing that the cells have TCR-independent effector functions. Especially, $CCR6^{high}$ MP $CD4^+$ T cells are major responders to IL-1β and IL-23 without MOG_{35-55} antigen reactivity, which gives them pathogenic-Th17 characteristics and allows them to contribute to autoimmune encephalomyelitis. We identified Bhlhe40 in $CCR6^{high}$ MP $CD4^+$ T cells drives the expression of GM-CSF, contributing to CNS pathology in experimental autoimmune encephalomyelitis. Collectively, our findings reveal heterogeneity of MP $CD4^+$ T cells that can contribute to autoimmune neuroinflammation in bystander manner synergistically with antigen-specific T cells.

Introduction

The immunological memory of antigen-specific T cells enables faster and more potent responses upon re-exposure to a previously encountered antigen, providing long-lasting immunity (Kaech & Cui, 2012). Although a substantial population of memory-phenotype (MP) conventional T cells exists in steady state mice unexposed to foreign antigens, it has been reported that MP T cells are formed before birth in humans and exist in germ-free (GF) and antigen-free (AF) conditioned mice (Byrne *et al*, 1994; Dobber *et al*, 1992; Haluszczak *et al*, 2009; Szabolcs *et al*, 2003).

After undergoing homeostatic proliferation in a lymphopenic environment, naïve T cells acquire phenotypical, functional, and gene expression–like antigen-specific memory and become MP T cells (Cho *et al*, 2000; Ernst *et al*, 1999; Goldrath & Bevan, 1999; Goldrath *et al*, 2004). T cell receptor (TCR) and CD28 signaling seem to be required for the conversion of naïve $CD4^+$ T cells into MP T cells. MP $CD4^+$ T cells express CD5, a marker with high affinity to self-antigen, and resist infection by mediating a Th1-like immune response without antigen stimulation (Kawabe *et al*, 2017). A previous study confirmed that antigen-non-specific MP $CD4^+$ T cells proliferated more than Lymphocytic choriomeningitis virus (LCMV)-specific T cells in an LCMV infection model. Indeed, treatment with an anti-MHCII antibody did not inhibit the proliferation of MP $CD4^+$ T cells, suggesting that they play a bystander role against infection (Younes *et al*, 2011).

Unlike MP $CD4^+$ T cells, MP $CD8^+$ T cells have been well studied for their antigen-specific and bystander functions. MP $CD8^+$ T cells can rapidly produce IFN-γ upon stimulation with IL-12 and IL-18 and without cognate antigen stimulation (Sosinowski *et al*, 2013; White *et al*, 2017). In particular, MP $CD8^+$ T cells are called virtual memory. They can have specific reactions to certain antigens without previous exposure (Akue *et al*, 2012; Haluszczak *et al.*, 2009; Hamilton *et al*, 2006; Sosinowski *et al.*, 2013; White *et al*, 2016) and increase NKG2D and granzyme B expression upon IL-12, IL-18, and IL-15 stimulation, producing a bystander killing role against infection (Chu *et al*, 2013; Lertmemongkolchai *et al*, 2001; White *et al.*, 2016). In addition, MP $CD8^+$ T cells can play an antigen-specific protection role in *Listeria monocytogenes*, Herpes simplex virus (HSV), and *vaccinia* infections (Haluszczak *et al.*, 2009; Hamilton *et al.*, 2006; Lee *et al*, 2013a; Sosinowski *et al.*, 2013). Also, MP $CD8^+$ T cells have high affinity to self-antigens, so they can break peripheral tolerance with MP $CD4^+$ T cells and develop autoimmune diabetes (King *et al*, 2004; Le Saout *et al*, 2008). Overall, previous studies have shown the function of MP $CD8^+$ T cells in disease, but the role of MP $CD4^+$ T cells in autoimmune disease has not yet been studied.

Most previous studies have focused on the role of autoantigen-specific T cells in both humans and mice to understand autoimmune diseases and find therapeutic drugs to regulate antigen-specific T cells (Serra & Santamaria, 2019). Interestingly, antigen-non-specific T cells, including myelin oligodendrocyte glycoprotein (MOG) tetramer–negative $CD4^+$ Th17 cells, also infiltrate the Central nervous system (CNS) in significant proportions and exacerbate experimental autoimmune encephalomyelitis (EAE) pathogenesis (Jones *et al*, 2003; Lee *et al*, 2019; Lees *et al*, 2010; Lin *et al*, 2016). In support, myelin-specific T cells were

found to be similar in Multiple sclerosis (MS) patients and healthy controls (Hellings *et al*, 2001; Hemmer *et al*, 1997). Bystander-activated T cells and Epstein-Barr virus–specific $CD8^+$ T cells are clonally expanded and correlate with disease pathogenesis in the joints of chronic inflammatory arthritis and Sjogren's syndrome patients (Brennan *et al*, 2008; Kobayashi *et al*, 2004; Tan *et al*, 2000), raising questions about the role of antigen-nonrelated T cells in autoimmune disease.

In this study, we hypothesized that MP conventional $CD4^+$ T cells could be encephalitogenic bystander cells during the development of autoimmune neuroinflammatory disease. First, we examined the heterogeneity of MP $CD4^+$ T cells using single cell RNA-sequencing (scRNA-seq) and TCR sequencing analyses. We found distinct subpopulations of Th1-, Th17-, Treg-, and Tfh-like cells among MP $CD4^+$ T cells. Those cells respond to IL-1 family cytokines and STAT activators, even without TCR stimulation. We further found that $CCR6^{high}$ MP $CD4^+$ T cells are the major responders to IL-1β and IL-23, expressing pathogenic signature genes in a bystander manner and thereby contributing to the development of MOG antigen–specific T cell–derived EAE. In this context, Bhlhe40 regulates the production of GM-CSF in $CCR6^{high}$ MP $CD4^+$ T cells, exacerbating EAE pathogenesis. Our findings indicate the pathogenic role of antigen-unrelated MP conventional $CD4^+$ T cells along with antigen-specific T cells during autoimmune neuroinflammatory disease.

Results

Single cell RNA-sequencing identifies distinct effector-like phenotypes in steady-state MP conventional $CD4^+$ T cells.

Steady-state, unprimed specific-pathogen-free (SPF)-housed mice have a significant proportion of MP $CD4^+$ T cells ($TCR\beta^+CD1d$ $tetramer^-CD8^-CD4^+CD25\text{-}CD44^{high}CD62L^{low}$) in their spleen, thymus, inguinal lymph nodes (iLNs), mesenteric lymph nodes (mLNs), Peyer's patches (PPs), and lung tissues (Fig. S1A and Fig. 1A). The proportion and number of $CD4^+$ T cells increased with age in all tissues (Fig. S1). To identify and focus on the characteristics of MP $CD4^+$ T cells, we used fluorescence-activated cell sorting (FACS) to sort MP $CD4^+$ T cells from the spleens of 10-week-old C57BL/6 mice and performed scRNA-seq with paired V(D)J sequencing of the T cell receptor (Fig. S2A to D). Also, we generated a pipeline to filter out PLZF and TCR $V_\alpha14\text{-}J_\alpha18$ (TRAV11-TRAJ18) expressing cells, a well-known key transcription factor for the development of NKT and MAIT cells (Koay *et al*, 2016; Kovalovsky *et al*, 2008; Savage *et al*, 2008). An unbiased clustering analysis revealed clearly distinct effector T cell–like subpopulations (Fig. 1B) and differentially expressed genes (DEGs) defining each cluster (Fig. 1C and D). A Gene Ontology (GO)/Kyoto Encyclopedia of Genes and Genomes (KEGG) analysis of each cluster indicated that clusters 3 and 5 were Th1- and Th17-like populations, respectively, with significance in "chemokine-mediated signaling pathway" and "cellular response to interleukin-1" (Fig. S3). In addition, lineage-specific transcription factors and chemokine receptors were localized in each cluster (Fig. 1E and Fig. S4), suggesting that MP $CD4^+$ T cells are composed of Th1-, Th17-, Tfh-, and Treg-like populations. To examine whether the subpopulations of steady-state MP $CD4^+$ T cells depended on germ or food antigens, we analyzed the proportion of $CD44^{high}CD62L^{low}$ MP $CD4^+$ T cells in the tissues of SPF-, GF-, and AF-housed mice using flow cytometry. The proportions of

total MP $CD4^+$ T cells were almost identical in the spleen and other tissues except the mLN and PP (Fig. 1F, Fig. S5A and S5B), indicating that the generation of splenic MP $CD4^+$ T cells is not affected by the microbiome or food antigen stimulation. Our scRNA-seq analysis further confirmed that the SPF- and GF-housed mice had identical proportions of distinct subpopulations of splenic MP $CD4^+$ T cells (Fig. 1G and 1H), but the proportion of Th17-like MP cells in the mLNs of GF-housed mice was much lower than that in the mLNs of SPF-housed mice (Fig. 1I and 1J). In support, the proportion of $CCR6^{high}$ or $ROR\gamma t^+$ MP $CD4^+$ T cells in the mLNs of GF-housed mice was lower than that in SPF-housed mice, suggesting that the generation of gut MP $CD4^+$ T cells is specifically dependent on germs (Fig. S6). The TCR clonal diversity of MP $CD4^+$ T cells in GF-housed mice, especially the Th17-like population in the mLNs, was reduced compared with SPF-housed mice, though comparable diversity was observed in the spleen (Fig. 1K and 1L). Together, these data indicate that steady-state splenic MP $CD4^+$ T cells contain heterogeneous subpopulations of Th1-, Th17-, Tfh-, and Treg-like cells that express effector molecules and exist independently of the gut microbiome and food antigens.

Phenotypic differences of MP $CD4^+$ T cells after exposure to IL-1 family and STAT activating cytokines.

To determine the effector functions of MP $CD4^+$ T cells to respond to various cytokines, we performed scRNA-seq of MP $CD4^+$ T cells cultured in conditioned medium with IL-12/IL-18, IL-25/IL-33, and IL-1β/IL-23 cytokines (Fig. 2A and Fig. S2E). Additionally, IL-7 was added to the culture medium for T-cell survival and maintenance (Kondrack *et al*, 2003). The merged Uniform Manifold Approximation and Projection (UMAP) plot shows phenotypic characteristics of Th1-, Th2-, Th17-, and Treg-like subpopulations (Fig. 2B and C), which express lineage specific genes (Fig. 2D). Each cytokine set induced distinct subpopulations localized exclusively in the plot (Fig. 2E). We further confirmed the expression of selected gene sets related to the Th1, Th2, and Th17 lineages in each bystander-activated condition, which shows that type 1, 2, and 3 cytokines can upregulate lineage-specific genes in MP $CD4^+$ T cells (Fig. 2F and G). A single-cell regulatory network inference and clustering (SCENIC) analysis in each cytokine condition revealed a significant level of common or specific transcription factor activity (Fig. 2H). In addition, an Ingenuity pathway analysis (IPA) showed the predicted transcriptional regulators in each condition and speculated that the target transcription factors included Bhlhe40, which can be a potent regulator of bystander activation in MP $CD4^+$ T cells (Fig. 2I). To evaluate the effector functions of MP $CD4^+$ T cells, we treated MP $CD4^+$ T cells with those cytokines and/or anti-CD3/anti-CD28 (Fig. 2J and 2K). Consistently, the MP $CD4^+$ T cells responded to IL-12/IL-18, IL-25/IL-33, and IL-1β/IL-23 cytokines without TCR stimulation, and T-bet^+ IFN-γ^+, $GATA3^+IL\text{-}13^+$, and $ROR\gamma t^+IL\text{-}17^+$ cells increased compared to TCR-stimulated condition (Fig. 2J). However, TNF-α was produced only in the presence of TCR stimulation and IFN-γ in the culture supernatant from IL-12/IL-18-conditioned MP $CD4^+$ T cells, and IL-4 was also significantly detected with TCR stimulation but not in the bystander condition with IL-25/IL-33. Similarly, Granulocyte-macrophage colony-stimulating factor (GM-CSF) was secreted more efficiently with IL-1β/IL-23 and TCR stimulation than with the cytokines alone (Fig. 2K). Collectively, these results indicate that MP $CD4^+$ T cells have functional heterogeneity when responding to specific sets of IL-1 family and STAT activators in the absence of their

cognate antigen and suggest possible potent transcriptional regulators that control MP $CD4^+$ T cell effector functions.

Potential responder MP $CD4^+$ T cells express distinct chemokine receptors upon IL-12/IL-18 and IL-1β/IL-23 stimulation.

To determine which MP $CD4^+$ T cells are potential responders to IL-1 family and STAT activating cytokines, we analyzed the subpopulation of expanding or responding clusters and performed trajectory analyses. Control MP $CD4^+$ T cells cultured with IL-7 produced a significantly separate population of $CXCR3^{high}$ cells. In IL-18/IL-12-conditioned MP $CD4^+$ T cells the $CXCR3^{high}$ cell population was reduced, and the IFN-γ- or IL-13^{high}expressing Th1 and proliferating Th1 populations were greatly increased (Fig. 3A and 3B). Th1 signature genes, *Tbx21, Ifng, Cxcr3, Il2rb1, Il18r1,* and *CCR5* were highly expressed by IL-18/IL-12-conditioned MP $CD4^+$ T cells (Fig. 3C). GO/KEGG analysis indicated that the related gene sets in those cells had increased including "Cellular response to interferon-gamma", "Cytokine cytokine receptor interaction", "Alzheimer's disease", and "Parkinson's disease" (Fig. 3D). The IPA returned terminologies related to cytokines and inflammation such as "JAK/STAT signaling" and "neuroinflammation signaling pathway" and related to cytotoxic response including "Granzyme B signaling" (Fig. 3E). In a pseudo-time trajectory analysis, the MP $CD4^+$ T cells formed a continuous progression that started in $CXCR3^{high}$ cells and gradually progressed toward Fate 1, which expressed *Ifng, Stat5a, Bhlhe40, Batf3, Irf4* and *Irf8* (Fig. 3F and 3G). Similarly, a $CCR6^{high}$ cluster was present in IL-7-conditioned MP $CD4^+$ T cells, and its Th17-like cluster was specifically increased by IL-1β and IL-23 (Fig. 3H and 3I). Th17 signature genes, *Rorc, Ccr6, Il17a Il1r1, Il23r*, and proliferating marker *Mki67* were expressed by those cells (Fig. 3J). GO/KEGG analysis predicted that the related gene sets in IL-1β /IL-23-cultured MP $CD4^+$ T cells had increased "Alzheimer's disease," "Parkinson's disease," and "Huntington's disease" which are neurological diseases and also increased "cytokine signaling pathway" (Fig. 3K). The IPA more clearly explained the related pathways, "STAT3 pathway," "leukocyte extravasation signaling," "neuroinflammation signaling pathway," "chemokine signaling," and "Th17 activation pathway" (Fig. 3L). In the trajectory analysis, $CCR6^{high}$ cells seemed to be the starting point, and then the cells gradually differentiated toward Fate 2 (Fig. 3M), which expresses pathogenic Th17-related genes such as *Rorc, Il17a, Csf2, Il22, Bhlhe40, Rora and Cebpb* with increased activities (Fig. 3N) and expression level (Fig. 3O) of related transcriptomes. These results collectively reveal that Th1-like and Th17-like MP $CD4^+$ T cells expressing different chemokine receptors respond specifically to IL-12/IL-18 and IL-1β/IL-23 cytokines with the effector functions.

$CCR6^{high}$ memory phenotype $CD4^+$ T cells are bystander-activated by IL-1β and IL-23 to become pathogenic Th17-like cells.

Since scRNA-seq predicted that $CCR6^{high}$ cells were the major cells responding to IL-1β and IL-23, we sorted splenic $CCR6^{high}$ and $CCR6^{low}$ MP $CD4^+$ T cells (Fig. 4A and 4B) and then determined their proportions in steady-state SPF- and GF-housed mice (Fig. 4C). We found that splenic $CCR6^{high}$ MP $CD4^+$ T cells were independent of the gut (Fig. 4C). $CCR6^{high}$ MP $CD4^+$ T cells expressed RORγt more highly than $CCR6^{low}$ cells

and had comparable expression of T-bet (Fig. 4D and 4E). Steady-state CCR6^{high} MP CD4^{+} T cells, but not CCR6^{low}, expressed IL-17A (Fig. 4F and 4G), suggesting that CCR6^{high} MP CD4^{+} T cells are Th17-like cells. Further stimulation by IL-1β and IL-23 induced IL-17A and GM-CSF expression (Fig. 4H and 4I), which confirms that CCR6^{high} MP CD4^{+} T cells produce pathogenic cytokines in the bystander manner. The amount of cytokine secreted, as determined by ELISA, consistently showed that CCR6^{high} MP CD4^{+} T cells, but not CCR6^{low}, significantly produced IL-17A, GM-CSF, and IFN-γ and that IL-1β and IL-23 had important synergy for pathogenicity (Fig. 4J). In addition, IL-1β greatly expanded RORγt expression in CCR6^{high} MP CD4^{+} T cells but not CCR6^{low} cells, whereas IL-23 somewhat inhibited the proportion of Ki67-expressing cells, suggesting that IL-1β is important for the proliferation of CCR6^{high} MP CD4^{+} T cells (Fig. 4K). To further confirm the functions of IL-1β and IL-23 in MP CD4^{+} T cells, we performed bulk-RNA seq with bystander-activated MP CD4^{+} T cells exposed to IL-1β and IL-23. In the heatmap DEG analysis, IL-1β increased the expression of proliferation-related gene such as *Mki67* and *cdk2*, whereas IL-23 alone did not have any significant effects on gene expression (Fig. 4L). IL-23 and IL-1β together significantly induced the expression of pathogenic genes such as *Bhlhe40*, *Il1r1*, *Csf2*, *Ifng*, *Il22* and *Il17a*. In support, Gene set enrichment analysis (GSEA) pathway enrichment plot of IL-1β vs. IL-1β and IL-23 demonstrated that the enrichment score for cell proliferation was higher with IL-1β, and the score of the pathogenic Th17 signature with IL-1β and IL-23 was higher than in the control group (Fig. 4M). Through these results, we understand that steady-state CCR6^{high} MP CD4^{+} T cells, which show Th17-like characteristics, are the major bystander-activated cells responding to IL-1β and IL-23, which potentiate the cells' pathogenic character.

CCR6^{high} MP CD4^{+} T cells are encephalitogenic and exacerbate autoimmune neuroinflammation.

To reveal the importance of splenic MP CD4^{+} T cells during an autoimmune disease, we first induced EAE in 5-week-old mice, who have a lower proportion of MP CD4^{+} T cells than 10-week-old mice. In this mouse model, we compared the disease severity of control mice with that of those who received an additional adoptive transfer of Treg-deleted MP CD4^{+} T cells from 10-week-old Foxp3-GFP mice. EAE was rapidly induced and progressed by transferring additional MP CD4^{+} T cells from 10-week-old mice, suggesting that MP CD4^{+} T cells could be an important contributor to MOG$_{35-55}$-induced EAE pathogenesis (Fig. S7A). In support, Rag$^{-/-}$ mice that received MOG-TCR transgenic (2D2) naïve CD45.1^{-}V$_{\beta}$11^{+}CD4^{+} T cells with Treg-deleted MP CD4^{+} T cells (CD45.1^{+}CD4^{+}) showed a more severe phenotype of EAE than the mice that received only 2D2 T cells (Fig. S7B), suggesting that MP CD4^{+} T cells contribute to the pathogenesis of EAE. Based on our previous results, we hypothesized that CCR6^{high} MP CD4^{+} T cells are the major pathogenic subpopulation contributing to EAE disease progression. To test that hypothesis, we transferred CCR6^{high} and CCR6^{low} MP CD4^{+} T cells (CD45.1^{+}CD4^{+}) and 2D2 naïve CD4^{+} T cells into Rag$^{-/-}$ mice. The additional transfer of CCR6^{high} MP CD4^{+} T cells exacerbated EAE development compared with 2D2 transfer alone or the transfer of CCR6^{low} MP CD4^{+} T cells (Fig. 5A). Interestingly, the number of transferred MP CD4^{+} T cells that appeared in the spinal cord and brain tissue did not differ between conditions (Fig. 5B). However, CCR6^{high} MP CD4^{+} T cells produced significantly more cytokines, particularly IL-17A and GM-CSF, in the spinal cord and brain tissue than CCR6^{low} MP CD4^{+} T cells (Fig. 5C and D). Therefore, CCR6^{high} MP CD4^{+} T cells, along

with antigen-specific T cells, contribute to the pathogenicity of autoimmune neuroinflammation by expressing pathogenic cytokines such as IL-17A and GM-CSF. To clarify the antigen-independent activation of CCR6^{high} MP CD4^{+} T cells in an EAE mouse model, we detected 2D2 TCR ($V_{\alpha}3.2^{+}$ and $V_{\beta}11^{+}$), which are predominantly expressed in 2D2 naïve CD4^{+} T cells. Indeed, CCR6^{high} MP CD4^{+} T cells barely expressed $V_{\alpha}3.2^{+}$ and $V_{\beta}11^{+}$ (Fig. 5E and F). In support, we confirmed that steady-state MP CD4^{+} T cells did not respond to the MOG_{35-55} antigen (Fig. 5G). Collectively, these results suggest that CCR6^{high} MP CD4^{+} T cells are encephalitogenic cells that exacerbate autoimmune neuroinflammation by producing IL-17A and GM-CSF, presumably in a bystander manner, along with antigen-specific T cells.

Bhlhe40 confers pathogenic functions of bystander CCR6^{high} MP CD4^{+} T cells by IL-1 and IL-23

Among the candidate genes involved in bystander activation of CCR6^{high} MP CD4^{+} T cells, we identified that Bhlhe40/GM-CSF axis could potentially give rise to the pathogenic function of CCR6^{high} MP CD4^{+} T cells induced by IL-1β and IL-23 without TCR stimulation (Fig. 6A). By using Bhlhe40^{GFP} mice, we found that CCR6^{high} MP CD4^{+} T cells activated by IL-1β and IL-23 showed significantly increased level of Bhlhe40 (Fig. 6B). Interestingly, Bhlhe40^{GFP} positive T cells majorly produced effector cytokines including IL-17A and GM-CSF compared to Bhlhe40^{GFP} negative T cells (Fig. 6C). In support, Bhlhe40$^{-/-}$ CCR6^{high} MP CD4^{+} T cells showed markedly reduced IL-17A and GM-CSF production compared to WT (Fig. 6D and E), suggesting that Bhlhe40 is an important transcriptional regulator for the pathogenic functions of bystander CCR6^{high} MP CD4^{+} T cells. To confirm the in vivo relevance, we transferred WT CCR6^{high} or Bhlhe40$^{-/-}$ CCR6^{high} MP CD4^{+} T cells along with 2D2 naïve CD4^{+} T cells into Rag$^{-/-}$ mice. Bhlhe40$^{-/-}$ CCR6^{high} MP CD4^{+} T cells showed abrogated functions for exacerbating EAE disease compared by WT CCR6^{high} MP CD4^{+} T cells (Fig. 6F). Interestingly, the number of Bhlhe40$^{-/-}$ CCR6^{high} MP CD4^{+} T cells expressing IL-17A and GM-CSF in the spinal cord and brain tissue was significantly reduced compared to WT CCR6^{high} MP CD4^{+} T cells (Fig. 6G and H) without significant difference of MOG-specific 2D2 T cells (data not shown). In addition, transfer of GM-CSF-deficient CCR6^{high} MP CD4^{+} T cells showed abrogated function of contributing EAE pathogenesis (Fig. 6I), suggesting that disease aggravation by bystander CCR6^{high} MP CD4^{+} T cells is committed by IL-1β and IL-23 via Bhlhe40/GM-CSF axis. Collectively, these results indicate that Bhlhe40 confers pathogenic functions of bystander CCR6^{high} MP CD4^{+} T cells with GM-CSF production.

Discussion

In this study, we intensively validated the characteristics of MP conventional CD4^{+} T cells using scRNA-seq to unveil their effector functions during autoimmune disease. We found distinct effector-like subpopulations in steady-state splenic MP CD4^{+} T cells that are independent of the microbiome and food antigens. Moreover, MP CD4^{+} T cells can be bystander-activated toward Th1-, Th2-, and Th17-like effector cells by the IL-1 family and STAT activating cytokines. In particular, chemokine receptor–expressing cells are defined as potential responder cells, and we focused on CCR6^{high} MP CD4^{+} T cells to further validate their functions in responding to IL-1β/IL-23. We demonstrated that encephalitogenic CCR6^{high} MP conventional CD4^{+} T cells are bystanders that exacerbate EAE disease progression, along with antigen-specific T cells. Furthermore, we

suggested Bhlhe40 as a pivotal transcriptional regulator that governs GM-CSF production by CCR6^{high} MP CD4^{+} T cells, exacerbating EAE development. Overall, our results reveal the immunological function of antigen-unrelated MP CD4^{+} T cells in autoimmune disease.

According to previous reports, CD44^{high} MP CD4^{+} and CD8^{+} conventional T cells exist spontaneously in mouse spleens, independently of germ and food antigens, and also in humans (Byrne *et al.*, 1994; Haluszczak *et al.*, 2009; Kawabe *et al.*, 2017; Szabolcs *et al.*, 2003). In support, we and others confirmed that MP CD4^{+} T cells are found in mice even 1-2 days after birth and that they increase significantly with age in both the spleen and other tissues (Kawabe *et al.*, 2017). However, the generation of MP CD8^{+} T cells remains controversial. Some studies have reported that MP CD8^{+} T cells are derived from naïve T cells in lymphopenic conditions (Haluszczak *et al.*, 2009; Hamilton *et al.*, 2006; Seddon *et al*, 2000; White *et al.*, 2016), whereas other groups have shown that MP CD8^{+} T cell generation is a TCR-related process triggered by the recognition of self-antigens in the thymus (Miller *et al*, 2020). Along the same lines, MP CD4^{+} T cells have recently been reported to differentiate from naïve CD4^{+} T cells in the periphery in both neonates and adult mice in a thymus-independent fashion (Kawabe *et al.*, 2017). However, it has been recently reported that there is a proportion of memory CD4^{+} T cells in human thymus by scRNA-seq (Park *et al*, 2020), suggesting the potential generation of natural MP T cells. In support, we observed a significant proportion and number of CD44^{high} MP CD4^{+} T cells in the mouse thymus that increased with age. Collectively, therefore, these studies do not rule out the possibility that MP CD4^{+} T cells might be generated both from naïve T cells and directly by the thymus. Furthermore, we found that the TCR diversity of steady-state MP CD4^{+} T cells was slightly reduced in GF mice, revealing that the gut microbiome potentially contributes to certain minor TCR clonotypes of peripheral MP CD4^{+} T cells. In the mLNs, Th17-like MP CD4^{+} T cells were significantly reduced in GF-housed mice, suggesting the importance of the microbiome to gut Th17 cells. Therefore, peripheral self-antigens and the gut microbiome might both contribute to TCR diversity and the proportion of MP CD4^{+} T cells.

The heterogeneous characteristics of MP conventional CD4^{+} T cells were investigated using single cell transcriptomics, which revealed clearly distinct Th1-, Th17-, Tfh-, and Treg-like subpopulations. In support, recent studies revealed the potential heterogeneity of murine MP CD4^{+} T cells (ElTanbouly *et al*, 2020; Kawabe *et al*, 2020) and further demonstrated that a CXCR3^{+}T-bet^{+} Th1-like MP population was differentiated from naïve CD4^{+} T cells by DC1-derived IL-12 and further activated by CD40–CD40L interactions between DC1 and CD4^{+} T cells (Kawabe *et al.*, 2020). Of note, MP CD4^{+} and CD8^{+} T cells rapidly produce IFN-γ in response to IL-12 and IL-18 (Guo *et al*, 2009; Kawabe *et al.*, 2017; Sosinowski *et al.*, 2013; White *et al.*, 2017). Given those observations, we hypothesized that CXCR3^{high} MP CD4^{+} T cells are major responders to IL-12 and IL-18 cytokine stimulation. As expected, we confirmed that CXCR3^{high} MP CD4^{+} T cells, in high correlation with CCR5 expression, can produce IFN-γ and T-bet in response to IL-12 and IL-18, suggesting a potential innate-like function of CXCR3^{high} MP CD4^{+} T cells. Interestingly, without TCR stimulation, cytokine-mediated bystander activation could not induce TNF-α from MP CD4^{+} T cells, suggesting that TCR and cytokine signaling produce distinct effector functions. We also used IL-33 and IL-25

stimulation of MP $CD4^+$ T cells to see whether they produced Th2 cytokines such as IL-13 and IL-5. Interestingly, the MP $CD4^+$ T cells produced IL-4 with TCR stimulation, suggesting that the effector function of MP $CD4^+$ T cells bystander-activated by IL-33 and IL-25 correlates with innate lymphoid cell type 2 (ILC2). A previous report consistently showed that *in vitro*–generated memory Th2 cells mainly produce IL-13, rather than IL-4, upon exposure to IL-33 and IL-7 without a cognate antigen. In addition, like ILC2, tissue-resident memory Th2 cells were activated by IL-33 and showed a protective function against helminth infection in an antigen-independent manner (Guo *et al*, 2015). Although we did not observe a significant Th2-like MP subpopulation in the steady state, we confirmed that Th2-like populations are induced by IL-33 and IL-25, suggesting that heterogeneous IL-33R- or IL-25R-expressing cells might be responding to those cytokines.

In our previous study, we demonstrated that and IL-23 can synergistically potentiate the pathogenicity of memory $CD4^+$ T cells *in vitro* (Lee *et al.*, 2019) and that non-myelin-specific $CD4^+$ T cells can infiltrate the CNS with MOG antigen–specific T cells, which significantly contribute to EAE disease progression (Jones *et al.*, 2003; Lee *et al.*, 2019). In rheumatoid arthritis patients, T cells that infiltrate the synovial fluid mainly express the $CD45RO^+$ memory marker and specifically respond to epitopes of Epstein-Barr virus and cytomegalovirus (Kobayashi *et al.*, 2004; Pacheco *et al*, 2019; Scotet *et al*, 1999; Tan *et al.*, 2000). In type 1 diabetes, infection with rotavirus or coxsackie virus is reported to be involved in accelerated diabetes onset through Toll-like receptor (TLR) signaling without pancreatic infection (Horwitz *et al*, 1998; Pane *et al*, 2014), and influenza A virus is linked to diabetes in human patients (Nenna *et al*, 2011; Pane & Coulson, 2015). Collectively, those studies suggest that antigen-non-related $CD4^+$ T cells can contribute to disease onset or progression with antigen-specific T cells in various autoimmune diseases. We have identified here that $CCR6^{high}$ MP $CD4^+$ T cells are the major subpopulation of MP $CD4^+$ T cells that respond to IL-1β and IL-23 by expanding and inducing pathogenic Th17 characteristics. In an adoptive transfer model of EAE, $CCR6^{high}$ MP $CD4^+$ T cells transferred with MOG-specific T cells induced more severe EAE than $CCR6^{low}$ cells, with increased production of IL-17 and GM-CSF in the CNS. We further confirmed that MP $CD4^+$ T cells do not respond to $MOG_{33\text{-}55}$ antigen, indicating the bystander role of $CCR6^{high}$ MP $CD4^+$ T cells in autoimmune neuroinflammation. Because MOG-specific T cells produce effector cytokines such as IL-17 and GM-CSF (data not shown), further studies should be done to reveal the distinct mechanism between antigen-specific T cells and bystander-activated T cells in autoimmune disease pathogenesis.

Analyzing the single cell transcriptomics of IL-1β/IL-23 responding MP $CD4^+$ T cells, we identified that Bhlhe40 could be a potential transcriptional regulator inducing GM-CSF in $CCR6^{high}$ MP $CD4^+$ T cells. Bhlhe40 has been reported to play pivotal roles in T cells. Bhlhe40-deficient naïve $CD4^+$ T cells show limited response to TCR stimulation (Martinez-Llordella *et al*, 2013). Moreover, Bhlhe40 seem to be required for Th1 and Th17 effector cytokine production including IL-17A, GM-CSF and IFN-γ in the context of autoimmune disease, GVHD, and Toxoplasma gondii infection model (Lin *et al.*, 2016; Lin *et al*, 2014; Piper *et al*, 2020; Yu *et al*, 2018). In addition, a binding site for Bhlhe40 was identified the correlation of mouse *Csf2* locus, which encodes GM-CSF, (Jarjour *et al*, 2020; Lin *et al.*, 2014) and Bhlhe40 expression positively correlate

with GM-CSF expression in human PBMC (Emming *et al*, 2020). We demonstrate that steady-state CCR6^{high} MP CD4^{+} T cells have Th17-like character with expressing RORγt. They up-regulated Bhlhe40 in response to IL-1β and IL-23 in the absence of TCR engagement for IL-17 and GM-CSF production. Moreover, transferring these cells in vivo, we found that Bhlhe40 is required in bystander CCR6^{high} MP CD4^{+} T cells for the expression of GM-CSF contributing to the pathogenesis of EAE development. In support, a previous study reported the majority of Bhlhe40-expressing pathogenic T cells in active EAE are non-MOG-specific (Lin *et al.*, 2016; Lin *et al.*, 2014). Therefore, Bhlhe40 can be a pivotal transcriptional regulator for both antigen-specific and bystander MP T cells in the context of CNS inflammation and targeting of Bhlhe40 in CD4^{+} T cells may serve as a potential novel treatment strategy to control autoimmune diseases.

Innate T cells such as natural killer T (NKT), mucosal-associated invariant T (MAIT), and γδ T cells have limited TCR gene usage compared to conventional T cells, which recognize complexes of non-peptide antigens such as glycolipids, phosphoantigens, and vitamin B metabolites, respectively (Godfrey *et al*, 2015; Lee *et al*, 2020; Pellicci *et al*, 2020). These innate T cells are derived from the thymus, which can evoke robust cytokine production. Previously, innate lymphocytes, such as NKT17, γδT17 cell, and ILC3 subsets have been defined to commonly express IL-17 and RORγt (Lee *et al*, 2013b; Sutton *et al*, 2009; Walker *et al*, 2013). Furthermore, a recent study reported a novel subset of αβ-γδ co-expressing T cells which recognize MHC-restricted peptide antigens and produce effector cytokine IL-17A, GM-CSF, and IFN-γ by IL-1β and IL-23 stimulation (Edwards *et al*, 2020). In this context, we carefully eliminated the possibility of contamination of innate T cells by sorting conventional MP CD4^{+} T cells using NKT (CD1d tetramer), γδ T, αβ-γδ T, ILC, and MAIT (TCRβ^{+}CD8^{-}CD4^{+}CD25^{-}CD44^{high}CD62L^{low}) exclusion gates. We confirmed that PLZF/CD1d tetramer negative steady-state MP CD4^{+} T cells still exists as a heterogenous population containing CCR6^{high}RORγt^{+}IL-17A^{+} cells, which is majorly bystander-activated by IL-1β and IL-23. Therefore, collectively, we provide compelling evidence that conventional CD4^{+} T cells distinguished from previously known innate T cells exist, which have an innate-like features and contribute to autoimmune neuroinflammation.

Memory T cells are antigen-experienced cells that respond to their cognate antigens more rapidly upon re-exposure. Therefore, we speculate that MP CD4^{+} T cells would have antigen-specific memory responses, and we wonder what the antigen is. Previous studies showed that antigen-specific cells called virtual memory cells exist without antigen exposure and nonetheless perform the memory response. For example, *vaccinia* virus B8R- and HSV-specific MP CD8^{+} T cells in unimmunized mice can react to those specific antigens (Haluszczak *et al.*, 2009; Hamilton *et al.*, 2006). Virtual memory CD8^{+} T cells have a CD44^{high}CD122^{+}CD49d^{low} phenotype which requires a transcription factor *Eomes* that differs from that of antigen-induced memory cells (Sosinowski *et al.*, 2013). In addition, virus-specific MP CD4^{+} T cells are abundant in unexposed adults, presumably through cross-reactivity, so that they have the typical properties of memory T cells (Su & Davis, 2013; Su *et al*, 2013). However, virtual memory CD8^{+} T cells are also known to play a protective role in infection using an antigen-non-specific manner (White *et al.*, 2016). Therefore, MP CD4^{+} T cells derived from steady-state mice might have cross-reactivity to certain pathogens even though

they did not respond to the MOG_{35-55} antigen *in vitro*, and we speculate that they have both antigen-specific and bystander functions.

Antigen-specific T cells are fundamentally important in triggering autoimmune inflammation; however, antigen-non-related MP $CD4^+$ T cells also contribute to pathogenic inflammation in a bystander manner. Collectively, our studies of the role that MP $CD4^+$ T cells play in neuroinflammatory disease shed light on the innate-like function of adaptive immune cells to understand disease pathogenesis and reveal a novel drug development strategy to modulate autoimmune diseases.

Experimental and Methods

Mice

C57BL/6J mice were purchased from DBL (Chungcheongbuk-do, Korea), and $Rag^{-/-}$, GM-$CSF^{-/-}$ and 2D2 TCR-transgenic mice were purchased from Jackson Laboratory (Bar Harbor, ME, USA). $CD45.1^+$, Foxp3-GFP mice were provided by Jeehee Youn (Hanyang University). GF and AF mice were purchased from the animal facility of POSTECH Biotech Center (Pohang, Korea). $Bhlhe40^{-/-}$ and $Bhlhe40^{GFP}$ mice were provided by Brian T. Edelson (Washington University). The mice were housed and bred in a specific pathogen–free animal facility at Hanyang University under controlled conditions with a constant temperature (21 ± 1 °C) and humidity (50 ± 5%) and a 12 h light/dark cycle with regular chow and autoclaved water.

Cell isolation and differentiation

MP ($TCR\beta^+CD4^+CD1d$ $tetramer^-CD25^-CD62L^{low}CD44^{high}$) $CD4^+$ T cells from the spleens of 8 to 12-week-old mice were isolated using a FACS Aria cell sorter II (BD Biosciences, Franklin Lakes, NJ, USA). FACS-sorted MP $CD4^+$ T cells were stimulated with IL-1β (20 ng/mL, R&D Systems, Minneapolis, MN, USA), IL-23 (20 ng/mL, R&D Systems), IL-12 (20 ng/mL, Peprotech, Rocky Hill, NJ, USA), IL-18 (20 ng/mL, R&D Systems), IL-33 (20 ng/mL, R&D Systems), IL-25 (20 ng/mL, R&D Systems), IL-7 (10 ng/mL, Peprotech, Rocky Hill, NJ, USA), or plate-bound anti-CD3/anti-CD28 (2 μg/mL, BD Biosciences) for 5 days at 37 °C in an incubator.

Flow cytometry

Cell surface staining was performed using the following monoclonal antibodies: anti-CD4 (RM4-5; eBioscience, San Diego, CA, USA, dilution 1:500), anti-CD25 (PC61.5; eBioscience, dilution 1:500), anti-CD44 (IM7; BioLegend, San Diego, CA, USA, dilution 1:500), anti-CD62L (MEL-14; BioLegend, dilution 1:500), anti-CD45 (30-F11, BioLegend, dilution 1:500), anti-CD45.1 (A20; eBioscience, dilution 1:500), anti-TCRβ (H57-597; eBioscience, dilution 1:500), anti-CCR6 (29-2L17; BD, dilution 1:100), anti-CXCR3 (CXCR3-173; BD, dilution 1:100), anti-$V_\alpha3.2$ (RR3-16; BioLegend, dilution 1:500), anti-$V_\beta11$ (RR3-15; BioLegend, dilution 1:500), and PE-conjugated CD1d tetramer (PBS57; NIH, dilution 1:1000). Biotinylated PBS57 loaded and unloaded CD1d monomers were provided by the US National Institutes of Health Tetramer

Core facility. For intracellular staining, the cells were stimulated with a cell stimulation cocktail (00-4975-03; eBioscience) for 4 h at 37 °C, and then surface markers were stained. After staining of the surface markers, the cells were fixed and permeabilized in Cytofix/Cytoperm (554714; BD Bioscience) or FOXP3/Transcription factor staining buffer set (00-5523-00; eBioscience) for 30 min at 4 °C or RT. Intracellular staining was performed using the following monoclonal antibodies: anti-IL-17A (eBio17B7; eBioscience, dilution 1:200), anti-IFN-γ (XMG1.2; eBioscience, dilution 1:400), anti-GM-CSF (MP1-22E9; BD Biosciences, dilution 1:200), anti-Ki67 (SolA15; eBioscience, dilution 1:500), anti-IL-4 (11B11; BioLegend, dilution 1:200), IL-13 (eBio13A; eBioscience, dilution 1:200), anti-TNF-α (MP6-XT22; BioLegend, dilution 1:500), anti-IL-5 (TRFK5; BioLegend, dilution 1:200), anti-IL-1R1 (35F5; BD Biosciences, dilution 1:100), anti-RORγt (Q31-378; BD Biosciences, dilution 1:100), anti-T-bet (4B10; BioLegend, dilution 1:50), anti-GATA3 (L50-823; BD Bioscience, dilution 3 μl per well) and IgG1 (R2-34; BD Biosciences). Stained cells were analyzed by flow cytometry (FACS Canto II, BD Bioscience), and data were analyzed using FlowJo software version 10.8.0 (Tree Star, Ashland, OR, USA).

Experimental autoimmune encephalomyelitis

In EAE model, FACS-sorted MP $CD4^+$ T cells ($TCR\beta^+CD4^+CD1d\ tetramer^-Foxp3^-CD62L^{low}CD44^{high}$, 5×10^5) from Foxp3-GFP mice were adoptively transferred to 5-week-old female C57BL/6 mice. After transfer, the mice were immunized with 200 μg of $MOG_{35\text{-}55}$ peptide in complete Freund's adjuvant (Chondrex, Inc., USA). At 0 and 48 h after immunization, the mice were intraperitoneally treated with 500 ng of pertussis toxin (List Biological Laboratories, Inc., Campbell, CA, USA). The animals were scored daily for clinical disease. In another EAE model by adoptive transfer, naive ($CD4^+V_\beta11^+CD25^-CD62L^{high}CD44^{low}$) $CD45.1^-$ T cells ($1\text{-}5 \times 10^4$) from 2D2 TCR-transgenic mice were transferred into $Rag^{-/-}$ mice with or without WT $CCR6^{high}$ or WT $CCR6^{low}$ or $Bhlhe40^{-/-}$ $CCR6^{high}$ or $GM\text{-}CSF^{-/-}$ $CCR6^{high}$ or $GM\text{-}CSF^{-/-}$ $CCR6^{low}$ MP $CD4^+$ T cells (1.0×10^5). Before transfer, $CCR6^{high}$ or $CCR6^{low}$ MP $CD4^+$ T cells were primed *in vitro* with IL-7 (10 ng/mL) and IL-1β (20 ng/mL) for 5–7 days. After transfer, the mice were immunized with 100 μg of MOG_{35-55} peptide in complete Freund's adjuvant (Chondrex, Inc., USA). At 0 and 48 h after immunization, the mice were intraperitoneally treated with 200 ng of pertussis toxin (List Biological Laboratories, Inc., Campbell, CA, USA). The animals were scored daily for clinical disease as follows (Stromnes & Goverman, 2006): partially limp tail, 0.5; completely limp tail, 1; limp tail and waddling gait, 1.5; paralysis of one hind limb, 2; paralysis of one hind limb and partial paralysis of the other hind limb, 2.5; paralysis of both hind limbs, 3; ascending paralysis, 3.5; paralysis of trunk, 4; moribund, 4.5; dead, 5. On day 12 or 13, the mice were sacrificed and perfused with Phosphate buffered saline (PBS). To isolate lymphocytes, the spinal cord and brain were digested with 1 mg/mL of collagenase D (11 088 866 001; Sigma-Aldrich) and DNase I (10 104 159 001; Sigma-Aldrich) and incubated at 80 RPM on a shaker for 35 min. After enzyme digestion, lymphocytes were isolated by Percoll (GE Healthcare, Little Chalfont, UK) density-gradient centrifugation.

T cell proliferation and cytokine assays

For antigen-specific proliferation, 2D2 naïve ($CD4^+V_\beta11^+CD25^-CD62L^{high}CD44^{low}$) and MP $CD4^+$ T cells ($CD4^+CD25^-CD62L^{low}CD44^{high}$) and $CD11c^+$ dendritic cells ($MHC\text{-}II^+CD11c^+$) (APC) from the spleens of 2D2 TCR-transgenic and C57BL/6 mice were isolated using a FACS Aria cell sorter II. Before co-culture, naïve and MP $CD4^+$ T cells were stained with 1.25 μM carboxyfluorescein succinimidyl ester (CFSE) (Invitrogen, Carlsbad, CA) for 7 min at room temperature. After incubation, 10% Fetal bovine serum (FBS) was added, and the incubation was continued on ice for 3 min. 2D2 Naïve and MP $CD4^+$ T cells (1×10^5 cells/well) were then washed with PBS and co-cultured with $CD11c^+$ dendritic cells (5×10^4) with or without 50 μg/mL of $MOG_{35\text{-}55}$ peptide for 72 h.

Enzyme-linked immunosorbent assay (ELISA)

Samples were measured using IL-17A ELISA (432501; BioLegend), IL-13 ELISA (88-7137-88; Thermo Fisher), IL-4 ELISA (431104; BioLegend), IL-5 ELISA (431204; BioLegend), IFN-γ ELISA (430801; BioLegend), TNF-α ELISA (430904; BioLegend), and GM-CSF ELISA (432201; BioLegend) kits according to the manufacturers' instructions. Briefly, microwell plates (Corning Costar; 9018) were coated with capture antibodies overnight at 4 °C and blocked with ELISA diluent 1X for 1 h at room temperature. Samples and two-fold serial diluted standards were incubated at room temperature for 2 h, and then detection antibodies and streptavidin-HRP were added. Then, 1X TMB solution and a stop solution (2 N H_2SO_4) was loaded. The optical density was analyzed at 450 nm. Between all procedures, plates were washed at least 3 times with wash buffer (1X PBS, 0.05% Tween-20).

Statistical analysis

All data were analyzed in non-parametric analyses using the Mann-Whitney test or two-way ANOVA of variance in Prism version 8.0 (GraphPad Software, San Diego, CA). Data are presented as the mean ± S.D. or mean ± S.E.M. For all data, significance was defined as $p \leq 0.05$. Sample size and statistical information is provided in each figure legend.

Single-cell RNA sequencing sample preparation

MP ($TCR\beta^+CD4^+CD25^-CD62L^{low}$ $CD44^{high}$) $CD4^+$ T cells from the spleens of 10-week-old mice were isolated using a FACS Aria cell sorter II (BD Biosciences, Franklin Lakes, NJ, USA). FACS-sorted MP $CD4^+$ T cells were stimulated with IL-1β (20 ng/mL, R&D Systems, Minneapolis, MN, USA), IL-23 (20 ng/mL, R&D Systems), IL-12 (20 ng/mL, Peprotech, Rocky Hill, NJ, USA), IL-18 (20 ng/mL, R&D Systems), IL-33 (20 ng/mL, R&D Systems), IL-25 (20 ng/mL, R&D Systems), or IL-7 (10 ng/mL, Peprotech, Rocky Hill, NJ, USA) for 5 days at 37 °C in an incubator.

Single-cell RNA- and TCR-seq data processing

Raw sequencing data were processed using a well-developed program, Cellranger (10X genomics), for quality control (QC) and gene expression estimation. Low-quality cells were filtered using 4 QC metrics: the

percentage of mitochondrial gene unique molecular identifier (UMI) counts, the number of expressed genes (UMI count > 0), the sum of UMI counts per cell, and the doublet score estimated using Doublet Finder [10.1016/j.cels.2019.03.003]. The outlier cells from each QC metric were excluded from further analyses. To collect pure TCRα/β$^+$ CD4$^+$ T cells, cells expressing PLZF (*Zbtb16*) and *Cd74*$^+$-cells in which at least 1 UMI was counted were removed. All TCRα/β$^+$ CD4$^+$T cells were integrated by cytokine treatment (set 1: IL-7, IL-7+ IL-1β, and IL-7+ IL-1β +IL-23; set 2: IL7, IL7+IL-25, IL-7+IL-33, and IL-7+IL-25+IL-33; set 3: IL-7, IL-7+IL-12, IL-7+IL-18, and IL-7+IL-12+IL-18) using monocle3 [10.1038/nmeth.4402]. TCR-seq raw sequencing data were processed using the Cellranger 'adj' program. The TCR clonotypes from previously filtered scRNA-seq were used in the further analyses.

Single-cell RNA-seq data analysis

The preprocessed scRNA-seq data were aligned with the IL-7 treatment group using 'align_cds' from the monocle3 program [https://doi.org/10.1038/s41586-019-0969-x], and data were integrated for each set. Each cluster was characterized using the marker gene expression levels and referring to previous studies. The top specifically expressed genes of each cluster were selected by the specificity of each gene, as estimated using 'FindAllMarkers' in Seurat v4.0 [https://doi.org/10.1016/j.cell.2021.04.048], and then their expression level was visualized using 'DoHeatmap' in the same program. We calculated the percentage of cells in each condition for each cell type by dividing the number of cells in each condition by the number of clustered cells. A DEGs analysis was performed for each cytokine treatment of each set using 'FindMarkers' in Seurat with the following parameters: min.pct = 0, min.cells.feature = 1, min.cells.group = 1, logfc.threshold = 0. DEGs between cytokine treatments and DEGs between conditions were defined at FDR <0.05 and average log2 fold change ≥0.1. A functional analysis of DEGs and cluster specific gene sets was performed in MSigDB's C2 (KEGG) and C5 (GO). The functions were analyzed using the maximum and minimum size of the gene sets (KEGG with min 2 genes and max 500, GO with min 2 genes and max 150 genes). The gene set enrichment test was performed using the 'enricher' function of the clusterProfile package [10.1089/omi.2011.0118]. The significance level was set as the function that satisfied FDR < 0.2 and had at least 2 overlapping genes.

Signature score of the MP CD4$^+$ T cells

The signature score of the CD4$^+$ T cells was estimated to define the features of each cell type. The monocle3 object of each set of cytokine treatments was transformed into the Seurat object. They were normalized by condition and then integrated. The signature score of each cell type was calculated using AddModuleScore in the Seurat package.

Trajectory inference of MP CD4$^+$ T cells by cytokine stimulation

Effector memory CD4$^+$ T-cells have the plasticity to differentiate into various helper cells. We performed a trajectory analysis on the subcluster composed of the initial cells that are likely to be differentiated according to each cytokine stimulus and the cells that responded. First, we selected 2,000 highly variable genes by cell type, and then we inferred the trajectory using reduceDimension with DDRTree in the monocle2 program

[10.1038/nbt.2859]. Pseudo-time was calculate using orderCells in the same program. DEGs following the pseudo-time trajectory were defined at a q-value < 1e-50.

Estimation of regulon activity score

Regulon describes the relationship between a transcription factor and its regulatory target genes, and its activity is calculated using the expression levels of the genes in the regulon. First, we constructed a correlation matrix between genes, and then we calculated the activity of each regulon using GENIE3 [10.1371/journal.pone.0012776]. At that time, all the parameters were set to the default. The regulon relationship was derived from mm10__refseq-r80__500bp_up_and_100bp_down_tss.mc9nr and mm10__refseq-r80__10kb_up_and_down_tss.mc9nr in the 'cisTarget_databases' of the R package. All processes were performed using the SCENIC program in R [10.1038/nmeth.4463]. Differentially activated regulons were considered only when they contained at least 1% of expressing cells.

T-cell receptor repertoire analysis

The TCR repertoire of the cells was considered only from the scRNA-seq data. The degree of TCR expansion was categorized as hyperexpanded (100 < X <= 500), large (20 < X <= 100), medium (5 < X <= 20), small (1 < X <= 5), and single (0 < X <= 1). The TCR diversity of each sample was calculated using Shannon's index, which considers non-uniformity in the frequency of the clonotype (gene and nucleotide sequences). All procedures were performed using scRepertoire [10.12688/f1000research.22139.2] in R.

SUPPLEMENTARY MATERIALS

Fig. S1. $CD44^{high}$ memory phenotype (MP) $CD4^{+}$ T cells increase with age in mice.

Fig. S2. Strategy and flow of single cell RNA-sequencing analysis.

Fig. S3. KEGG/GO analysis of steady-state MP $CD4^{+}$ T cells.

Fig. S4. Effector T cell lineage–specific marker expression in MP $CD4^{+}$ T cells.

Fig. S5. Comparison of MP $CD4^{+}$ T cells in tissues from SPF, GF, and AF mice.

Fig. S6. Effector T cell lineage–specific chemokine receptors and transcription factors in MP $CD4^{+}$ T cells from SPF and GF mice.

Fig. S7. MP $CD4^{+}$ T cells exacerbate autoimmune encephalomyelitis.

538 **REFERENCES AND NOTES**

539 Akue AD, Lee JY, Jameson SC (2012) Derivation and maintenance of virtual memory CD8 T cells. *J*
540 *Immunol* 188: 2516-2523
541 Brennan FM, Smith NM, Owen S, Li C, Amjadi P, Green P, Andersson A, Palfreeman AC, Hillyer P,
542 Foey A *et al* (2008) Resting CD4+ effector memory T cells are precursors of bystander-activated
543 effectors: a surrogate model of rheumatoid arthritis synovial T-cell function. *Arthritis Res Ther* 10:
544 R36
545 Byrne JA, Stankovic AK, Cooper MD (1994) A novel subpopulation of primed T cells in the human
546 fetus. *J Immunol* 152: 3098-3106
547 Cho BK, Rao VP, Ge Q, Eisen HN, Chen J (2000) Homeostasis-stimulated proliferation drives naive
548 T cells to differentiate directly into memory T cells. *J Exp Med* 192: 549-556
549 Chu T, Tyznik AJ, Roepke S, Berkley AM, Woodward-Davis A, Pattacini L, Bevan MJ, Zehn D, Prlic
550 M (2013) Bystander-activated memory CD8 T cells control early pathogen load in an innate-like,
551 NKG2D-dependent manner. *Cell Rep* 3: 701-708
552 Dobber R, Hertogh-Huijbregts A, Rozing J, Bottomly K, Nagelkerken L (1992) The involvement of
553 the intestinal microflora in the expansion of CD4+ T cells with a naive phenotype in the periphery.
554 *Dev Immunol* 2: 141-150
555 Edwards SC, Sutton CE, Ladell K, Grant EJ, McLaren JE, Roche F, Dash P, Apiwattanakul N, Awad
556 W, Miners KL *et al* (2020) A population of proinflammatory T cells coexpresses alphabeta and
557 gammadelta T cell receptors in mice and humans. *J Exp Med* 217
558 ElTanbouly MA, Zhao Y, Nowak E, Li J, Schaafsma E, Le Mercier I, Ceeraz S, Lines JL, Peng C,
559 Carriere C *et al* (2020) VISTA is a checkpoint regulator for naive T cell quiescence and peripheral
560 tolerance. *Science* 367
561 Emming S, Bianchi N, Polletti S, Balestrieri C, Leoni C, Montagner S, Chirichella M, Delaleu N,
562 Natoli G, Monticelli S (2020) A molecular network regulating the proinflammatory phenotype of
563 human memory T lymphocytes. *Nat Immunol* 21: 388-399
564 Ernst B, Lee DS, Chang JM, Sprent J, Surh CD (1999) The peptide ligands mediating positive
565 selection in the thymus control T cell survival and homeostatic proliferation in the periphery.
566 *Immunity* 11: 173-181
567 Godfrey DI, Uldrich AP, McCluskey J, Rossjohn J, Moody DB (2015) The burgeoning family of
568 unconventional T cells. *Nat Immunol* 16: 1114-1123
569 Goldrath AW, Bevan MJ (1999) Low-affinity ligands for the TCR drive proliferation of mature CD8+ T
570 cells in lymphopenic hosts. *Immunity* 11: 183-190
571 Goldrath AW, Luckey CJ, Park R, Benoist C, Mathis D (2004) The molecular program induced in T
572 cells undergoing homeostatic proliferation. *Proc Natl Acad Sci U S A* 101: 16885-16890
573 Guo L, Huang Y, Chen X, Hu-Li J, Urban JF, Jr., Paul WE (2015) Innate immunological function of
574 TH2 cells in vivo. *Nat Immunol* 16: 1051-1059

575 Guo L, Wei G, Zhu J, Liao W, Leonard WJ, Zhao K, Paul W (2009) IL-1 family members and STAT
576 activators induce cytokine production by Th2, Th17, and Th1 cells. *Proc Natl Acad Sci U S A* 106:
577 13463-13468
578 Haluszczak C, Akue AD, Hamilton SE, Johnson LD, Pujanauski L, Teodorovic L, Jameson SC, Kedl
579 RM (2009) The antigen-specific CD8+ T cell repertoire in unimmunized mice includes memory
580 phenotype cells bearing markers of homeostatic expansion. *J Exp Med* 206: 435-448
581 Hamilton SE, Wolkers MC, Schoenberger SP, Jameson SC (2006) The generation of protective
582 memory-like CD8+ T cells during homeostatic proliferation requires CD4+ T cells. *Nat Immunol* 7:
583 475-481
584 Hellings N, Baree M, Verhoeven C, D'Hooghe M B, Medaer R, Bernard CC, Raus J, Stinissen P
585 (2001) T-cell reactivity to multiple myelin antigens in multiple sclerosis patients and healthy controls.
586 *J Neurosci Res* 63: 290-302
587 Hemmer B, Vergelli M, Tranquill L, Conlon P, Ling N, McFarland HF, Martin R (1997) Human T-cell
588 response to myelin basic protein peptide (83-99): extensive heterogeneity in antigen recognition,
589 function, and phenotype. *Neurology* 49: 1116-1126
590 Horwitz MS, Bradley LM, Harbertson J, Krahl T, Lee J, Sarvetnick N (1998) Diabetes induced by
591 Coxsackie virus: initiation by bystander damage and not molecular mimicry. *Nat Med* 4: 781-785
592 Jarjour NN, Bradstreet TR, Schwarzkopf EA, Cook ME, Lai CW, Huang SC, Taneja R, Stappenbeck
593 TS, Van Dyken SJ, Urban JF, Jr. *et al* (2020) BHLHE40 Promotes TH2 Cell-Mediated Antihelminth
594 Immunity and Reveals Cooperative CSF2RB Family Cytokines. *J Immunol* 204: 923-932
595 Jones RE, Kay T, Keller T, Bourdette D (2003) Nonmyelin-specific T cells accelerate development
596 of central nervous system APC and increase susceptibility to experimental autoimmune
597 encephalomyelitis. *J Immunol* 170: 831-837
598 Kaech SM, Cui W (2012) Transcriptional control of effector and memory CD8+ T cell differentiation.
599 *Nat Rev Immunol* 12: 749-761
600 Kawabe T, Jankovic D, Kawabe S, Huang Y, Lee PH, Yamane H, Zhu J, Sher A, Germain RN, Paul
601 WE (2017) Memory-phenotype CD4(+) T cells spontaneously generated under steady-state
602 conditions exert innate TH1-like effector function. *Sci Immunol* 2
603 Kawabe T, Yi J, Kawajiri A, Hilligan K, Fang D, Ishii N, Yamane H, Zhu J, Jankovic D, Kim KS *et al*
604 (2020) Requirements for the differentiation of innate T-bet(high) memory-phenotype CD4(+) T
605 lymphocytes under steady state. *Nat Commun* 11: 3366
606 King C, Ilic A, Koelsch K, Sarvetnick N (2004) Homeostatic expansion of T cells during immune
607 insufficiency generates autoimmunity. *Cell* 117: 265-277
608 Koay HF, Gherardin NA, Enders A, Loh L, Mackay LK, Almeida CF, Russ BE, Nold-Petry CA, Nold
609 MF, Bedoui S *et al* (2016) A three-stage intrathymic development pathway for the mucosal-
610 associated invariant T cell lineage. *Nat Immunol* 17: 1300-1311

611 Kobayashi M, Yasui N, Ishimaru N, Arakaki R, Hayashi Y (2004) Development of autoimmune
612 arthritis with aging via bystander T cell activation in the mouse model of Sjogren's syndrome.
613 *Arthritis Rheum* 50: 3974-3984
614 Kondrack RM, Harbertson J, Tan JT, McBreen ME, Surh CD, Bradley LM (2003) Interleukin 7
615 regulates the survival and generation of memory CD4 cells. *J Exp Med* 198: 1797-1806
616 Kovalovsky D, Uche OU, Eladad S, Hobbs RM, Yi W, Alonzo E, Chua K, Eidson M, Kim HJ, Im JS
617 *et al* (2008) The BTB-zinc finger transcriptional regulator PLZF controls the development of invariant
618 natural killer T cell effector functions. *Nat Immunol* 9: 1055-1064
619 Le Saout C, Mennechet S, Taylor N, Hernandez J (2008) Memory-like CD8+ and CD4+ T cells
620 cooperate to break peripheral tolerance under lymphopenic conditions. *Proc Natl Acad Sci U S A*
621 105: 19414-19419
622 Lee HG, Lee JU, Kim DH, Lim S, Kang I, Choi JM (2019) Pathogenic function of bystander-activated
623 memory-like CD4(+) T cells in autoimmune encephalomyelitis. *Nat Commun* 10: 709
624 Lee JY, Hamilton SE, Akue AD, Hogquist KA, Jameson SC (2013a) Virtual memory CD8 T cells
625 display unique functional properties. *Proc Natl Acad Sci U S A* 110: 13498-13503
626 Lee M, Lee E, Han SK, Choi YH, Kwon DI, Choi H, Lee K, Park ES, Rha MS, Joo DJ *et al* (2020)
627 Single-cell RNA sequencing identifies shared differentiation paths of mouse thymic innate T cells.
628 *Nat Commun* 11: 4367
629 Lee YJ, Holzapfel KL, Zhu J, Jameson SC, Hogquist KA (2013b) Steady-state production of IL-4
630 modulates immunity in mouse strains and is determined by lineage diversity of iNKT cells. *Nat*
631 *Immunol* 14: 1146-1154
632 Lees JR, Sim J, Russell JH (2010) Encephalitogenic T-cells increase numbers of CNS T-cells
633 regardless of antigen specificity by both increasing T-cell entry and preventing egress. *J*
634 *Neuroimmunol* 220: 10-16
635 Lertmemongkolchai G, Cai G, Hunter CA, Bancroft GJ (2001) Bystander activation of CD8+ T cells
636 contributes to the rapid production of IFN-gamma in response to bacterial pathogens. *J Immunol*
637 166: 1097-1105
638 Lin CC, Bradstreet TR, Schwarzkopf EA, Jarjour NN, Chou C, Archambault AS, Sim J, Zinselmeyer
639 BH, Carrero JA, Wu GF *et al* (2016) IL-1-induced Bhlhe40 identifies pathogenic T helper cells in a
640 model of autoimmune neuroinflammation. *J Exp Med* 213: 251-271
641 Lin CC, Bradstreet TR, Schwarzkopf EA, Sim J, Carrero JA, Chou C, Cook LE, Egawa T, Taneja R,
642 Murphy TL *et al* (2014) Bhlhe40 controls cytokine production by T cells and is essential for
643 pathogenicity in autoimmune neuroinflammation. *Nat Commun* 5: 3551
644 Martinez-Llordella M, Esensten JH, Bailey-Bucktrout SL, Lipsky RH, Marini A, Chen J, Mughal M,
645 Mattson MP, Taub DD, Bluestone JA (2013) CD28-inducible transcription factor DEC1 is required
646 for efficient autoreactive CD4+ T cell response. *J Exp Med* 210: 1603-1619
647 Miller CH, Klawon DEJ, Zeng S, Lee V, Socci ND, Savage PA (2020) Eomes identifies thymic
648 precursors of self-specific memory-phenotype CD8(+) T cells. *Nat Immunol* 21: 567-577

649 Nenna R, Papoff P, Moretti C, Pierangeli A, Sabatino G, Costantino F, Soscia F, Cangiano G, Ferro
650 V, Mennini M *et al* (2011) Detection of respiratory viruses in the 2009 winter season in Rome: 2009
651 influenza A (H1N1) complications in children and concomitant type 1 diabetes onset. *Int J*
652 *Immunopathol Pharmacol* 24: 651-659
653 Pacheco Y, Acosta-Ampudia Y, Monsalve DM, Chang C, Gershwin ME, Anaya JM (2019)
654 Bystander activation and autoimmunity. *J Autoimmun* 103: 102301
655 Pane JA, Coulson BS (2015) Lessons from the mouse: potential contribution of bystander
656 lymphocyte activation by viruses to human type 1 diabetes. *Diabetologia* 58: 1149-1159
657 Pane JA, Webster NL, Coulson BS (2014) Rotavirus activates lymphocytes from non-obese diabetic
658 mice by triggering toll-like receptor 7 signaling and interferon production in plasmacytoid dendritic
659 cells. *PLoS Pathog* 10: e1003998
660 Park JE, Botting RA, Dominguez Conde C, Popescu DM, Lavaert M, Kunz DJ, Goh I, Stephenson
661 E, Ragazzini R, Tuck E *et al* (2020) A cell atlas of human thymic development defines T cell
662 repertoire formation. *Science* 367
663 Pellicci DG, Koay HF, Berzins SP (2020) Thymic development of unconventional T cells: how NKT
664 cells, MAIT cells and gammadelta T cells emerge. *Nat Rev Immunol* 20: 756-770
665 Piper C, Zhou V, Komorowski R, Szabo A, Vincent B, Serody J, Alegre ML, Edelson BT, Taneja R,
666 Drobyski WR (2020) Pathogenic Bhlhe40+ GM-CSF+ CD4+ T cells promote indirect alloantigen
667 presentation in the GI tract during GVHD. *Blood* 135: 568-581
668 Savage AK, Constantinides MG, Han J, Picard D, Martin E, Li B, Lantz O, Bendelac A (2008) The
669 transcription factor PLZF directs the effector program of the NKT cell lineage. *Immunity* 29: 391-403
670 Scotet E, Peyrat MA, Saulquin X, Retiere C, Couedel C, Davodeau F, Dulphy N, Toubert A, Bignon
671 JD, Lim A *et al* (1999) Frequent enrichment for CD8 T cells reactive against common herpes viruses
672 in chronic inflammatory lesions: towards a reassessment of the physiopathological significance of T
673 cell clonal expansions found in autoimmune inflammatory processes. *Eur J Immunol* 29: 973-985
674 Seddon B, Legname G, Tomlinson P, Zamoyska R (2000) Long-term survival but impaired
675 homeostatic proliferation of Naive T cells in the absence of p56lck. *Science* 290: 127-131
676 Serra P, Santamaria P (2019) Antigen-specific therapeutic approaches for autoimmunity. *Nat*
677 *Biotechnol* 37: 238-251
678 Sosinowski T, White JT, Cross EW, Haluszczak C, Marrack P, Gapin L, Kedl RM (2013) CD8alpha+
679 dendritic cell trans presentation of IL-15 to naive CD8+ T cells produces antigen-inexperienced T
680 cells in the periphery with memory phenotype and function. *J Immunol* 190: 1936-1947
681 Stromnes IM, Goverman JM (2006) Active induction of experimental allergic encephalomyelitis. *Nat*
682 *Protoc* 1: 1810-1819
683 Su LF, Davis MM (2013) Antiviral memory phenotype T cells in unexposed adults. *Immunol Rev*
684 255: 95-109
685 Su LF, Kidd BA, Han A, Kotzin JJ, Davis MM (2013) Virus-specific CD4(+) memory-phenotype T
686 cells are abundant in unexposed adults. *Immunity* 38: 373-383

Sutton CE, Lalor SJ, Sweeney CM, Brereton CF, Lavelle EC, Mills KH (2009) Interleukin-1 and IL-23 induce innate IL-17 production from gammadelta T cells, amplifying Th17 responses and autoimmunity. *Immunity* 31: 331-341

Szabolcs P, Park KD, Reese M, Marti L, Broadwater G, Kurtzberg J (2003) Coexistent naive phenotype and higher cycling rate of cord blood T cells as compared to adult peripheral blood. *Exp Hematol* 31: 708-714

Tan LC, Mowat AG, Fazou C, Rostron T, Roskell H, Dunbar PR, Tournay C, Romagne F, Peyrat MA, Houssaint E *et al* (2000) Specificity of T cells in synovial fluid: high frequencies of CD8(+) T cells that are specific for certain viral epitopes. *Arthritis Res* 2: 154-164

Walker JA, Barlow JL, McKenzie AN (2013) Innate lymphoid cells--how did we miss them? *Nat Rev Immunol* 13: 75-87

White JT, Cross EW, Burchill MA, Danhorn T, McCarter MD, Rosen HR, O'Connor B, Kedl RM (2016) Virtual memory T cells develop and mediate bystander protective immunity in an IL-15-dependent manner. *Nat Commun* 7: 11291

White JT, Cross EW, Kedl RM (2017) Antigen-inexperienced memory CD8(+) T cells: where they come from and why we need them. *Nat Rev Immunol* 17: 391-400

Younes SA, Punkosdy G, Caucheteux S, Chen T, Grossman Z, Paul WE (2011) Memory phenotype CD4 T cells undergoing rapid, nonburst-like, cytokine-driven proliferation can be distinguished from antigen-experienced memory cells. *PLoS Biol* 9: e1001171

Yu F, Sharma S, Jankovic D, Gurram RK, Su P, Hu G, Li R, Rieder S, Zhao K, Sun B *et al* (2018) The transcription factor Bhlhe40 is a switch of inflammatory versus antiinflammatory Th1 cell fate determination. *J Exp Med* 215: 1813-1821

Acknowledgements

We thank Dr. Dongsoo Kyeong and Dr. Younhee Shin (Insilicogen Inc.) for supporting bioinformatic analysis of the scRNA-seq data. We thank Mr. Yeon-Ho Kim and Ms. In Young Song for technical support in the FACS sorting conducted at Hanyang LINC Analytical Equipment Center (Seoul) and the NIH tetramer core facility (Emory University) for providing mouse CD1d PBS-57 (Biotinylated Monomer). We thank Prof. Jeehee Youn (Hanyang University) for kindly providing CD45.1^{+}, Foxp3-GFP mice and Prof. Kwang Soon Kim (POSTECH) for helping us purchase germ-free and antigen-free mice.

Funding

This research was supported by the Basic Science Research Program (NRF-2019R1A2C3006155) of the National Research Foundation funded by the Korean government.

Author contributions

M.-Z.C., H.-G.L., and J.-M.C. conceptualized and designed this study. M.-Z.C., H.-G.L. performed and analyzed most of the experiments including bioinformatic analysis. Y.J.L. supported conceptualization for bioinformatic analyses. J.-W.Y., G.-R.K. and J.-H.K. supported experiments. R.T. and B.T.E. provided Bhlhe40$^{-/-}$ and Bhlhe40^{GFP}. M.-Z.C., H.-G.L., and J.-M.C. wrote draft manuscript, and all authors reviewed the manuscript. J.-M.C. supervised the analyses and acquired funding.

Conflict of Interest

The authors declare that they have no competing interests.

Data and materials availability

The data that support the findings of this study are available from the corresponding author upon reasonable request. RNA-seq data have been deposited in the NCBI Gene Expression Omnibus.

Figures

Figure 1. Single cell RNA-sequencing identifies distinct effector-like phenotypes in steady-state MP CD4$^+$ T cells. (A) Representative flow cytometry plots showing the population of memory-phenotype (MP) CD4$^+$ T cells (TCRβ$^+$CD1d tetramer$^-$CD8$^-$CD4$^+$CD25$^-$CD62L^{low}CD44^{high}) in murine spleens, thymuses, inguinal lymph nodes (iLNs), lungs, mesenteric lymph nodes (mLNs), and Peyer's patches (PP). (B) tSNE plot of splenic MP CD4$^+$ T cells isolated from 10-week-old specific-pathogen-free (SPF) mice. (C) Heatmap of differentially expressed transcripts in splenic MP CD4$^+$ T cells. (D) Expression of selected genes used to define MP CD4$^+$ T cell clusters. (E) Differential expression of transcription factors and chemokine receptors from splenic MP CD4$^+$ T cell clusters. (F) Flow cytometry plots of splenic MP CD4$^+$ T cells (TCRβ$^+$CD1d tetramer$^-$CD8$^-$CD4$^+$CD25$^-$CD62L^{low}CD44^{high}) from SPF-, GF-, and AF-mice. (G) tSNE plot and (h) proportion of integrated splenic MP CD4$^+$ T cells isolated from 10-week-old SPF- and GF-mice. (I) tSNE plot and (J) proportion of integrated mLN MP CD4$^+$ T cells isolated from SPF- and GF-mice. (K) Pie chart representing the clonal size distribution of MP CD4$^+$ T cells. (L) Diversity of the TCR repertoire in MP CD4$^+$ T cell subsets from SPF- and GF-mice.

Figure 2. Phenotypic differences of MP CD4$^+$ T cells after exposure to IL-1 family and STAT activating cytokines. (A) Overview of experimental design. (B) UMAP representation of MP CD4$^+$ T cells stimulated with IL-12 and/or IL-18 and IL-33 and/or IL-25 and IL-1β and/or IL-23 in the presence of IL-7. (C) Heatmap and (D) violin plots of differentially expressed transcripts in cluster. (E) Individual cytokines conditions visualized with UMAP. (F) MA plots of differentially expressed genes comparing IL-7 versus IL-12/18 or IL-33/25 or IL-1β/23. (G) Heatmap representing gene expression of Resting-, Tfh-, Th1-, Th2-, Th17- and Treg-related gene signatures in each cytokine condition. (H) Heatmap representing transcription activity. (I) Venn diagram of transcriptional regulators predicted by the IPA. Numbers indicate the number of gene in each gate. (J) MP CD4$^+$ T cells (TCRβ$^+$CD1d tetramer$^-$CD8$^-$CD4$^+$CD25$^-$CD62L^{low}CD44^{high}) were cultured for 5 days with IL-12 and/or IL-18 and IL-33 and/or IL-25 and IL-1β and/or IL-23 in the presence of IL-7 or anti-

CD3/anti-CD28. Representative flow cytometry plots showing the expression of effector lineage markers in each cytokine condition. (K) IFN-γ, TNF-α, IL-4, IL-5, IL-13, IL-17A, and GM-CSF were measured by ELISA (n=5). Data are presented as the mean ± S.D. P values were calculated using Mann-Whitney U-test (*p < 0.05, **p < 0.01, ***p < 0.001).

Figure 3. Potential responder MP CD4$^+$ T cells express distinct chemokine receptors upon IL-12/IL-18 and IL-1β /IL-23 stimulation. (A) tSNE plots and (B) proportion of MP CD4$^+$ T cells stimulated with IL-12 and IL-18 in the presence of IL-7 for 5 days. (C) Expression of selected Th1-related genes. (D) Selected KEGG/GO terms in cluster 2,3,4 and 6 and (E) Ingenuity pathway analysis (IPA) in cluster 3,4 and 6 of IL-12- and IL-18-responded MP CD4$^+$ T cells. (F) Pseudo-time trajectory: each cell is colored by its pseudo-time value and (G) the expression level of the related genes. (H) tSNE plots and (I) proportion of MP CD4$^+$ T cells stimulated with IL-1β and IL-23 in the presence of IL-7 for 5 days. (J) Expression of selected Th17-related genes. (K) Selected KEGG/GO terms and (L) IPA of IL-1β- and IL-23-stimulated MP CD4$^+$ T cells (clusters 3, 4, 6). (M) Pseudo-times trajectory: each cell is colored by its pseudo-time value and (N) the transcription factor activity and (O) expression level of the related genes.

Figure 4. CCR6^{high} MP CD4$^+$ T cells are bystander-activated by IL-1β and IL-23 to become pathogenic Th17-like cells. (A) Gating strategy of CCR6^{high} and CCR6^{low} MP CD4$^+$ T cells from SPF mice. (B) The percentage of CCR6 expression in steady-state splenic MP CD4$^+$ T cells (n=6). (C) The expression of CCR6 in SPF- vs. GF-MP CD4$^+$ T cells (n=4). (dD) Transcription factor expression level of T-bet and RORγt in FACS-sorted CCR6^{high} and CCR6^{low} MP CD4$^+$ T cells and (E) the proportion (n=4). (F) Representative flow cytometry plots showing the cytokine expression and (G) the average proportion of CCR6^{high} MP CD4$^+$ T cells vs. CCR6^{low} MP CD4$^+$ T cells (n = 6). CCR6^{high} and CCR6^{low} MP CD4$^+$ T cells were stimulated with IL-1β and/or IL-23 in the presence of IL-7 for 5 days. (H) The representative proportion and (I) the average value showing the cytokine producing cells (n=5). (J) Concentration of IL-17A, GM-CSF, and IFN-γ were analyzed by ELISA (n = 5). (K) The proportion of RORγt$^+$ and Ki67$^+$ cells in CCR6^{high} and CCR6^{low} MP CD4$^+$ T cells. (L) Heatmap of selected genes (M) Gene set enrichment analysis (GSEA) pathway enrichment plot related to "Cell Proliferation" and "Pathogenic T_H17 signature" by bulk RNA-seq analysis. *q*, false discovery rate; NES, normalized enrichment score. Data are presented as the mean ± S.D. All data of p values were calculated using Mann-Whitney U-test (ND, not detected; NS, not significant; *p < 0.05, **p < 0.01, ***p < 0.001).

Figure 5. CCR6^{high} MP CD4$^+$ T cells are encephalitogenic and exacerbate autoimmune neuroinflammation. (A) Naïve CD4$^+$ T cells (5×10^4) from 2D2 transgenic mice were adoptively transferred, with or without CCR6^{high} or CCR6^{low} MP CD4$^+$ T cells (1×10^5 CD45.1$^+$TCRβ$^+$CD1d tetramer$^-$CD4$^+$CD25$^-$ CD62L^{low}CD44^{high}), into Rag$^{-/-}$ mice who were immunized with MOG_{35-55} in CFA. EAE clinical score was monitored daily (n=15). (B) Absolute cell numbers of infiltrated CD45.1$^+$MP CD4$^+$ T cells in the spinal cord and brain (n=8). (C) The representative plots and (D) absolute cell number of IL-17A, GM-CSF, and IFN-γ producing cells were determined in MP CD4$^+$ T cells from the spinal cords and brains on days 12–13 after immunization (n=8). (E) The representative dot plots and (F) the average value showing the percentage of 2D2 TCR ($V_\alpha3.2^+$ and $V_\beta11^+$) in spleens from 2D2 transgenic mice and C57BL/6 wild type mice (n=4). (G)

FACS-sorted 2D2 naïve $CD4^+$ T cells and MP $CD4^+$ T cells were cultured with $CD11c^+$ dendritic cells (MHC-II^+CD11c^+) with or without MOG_{35-55} peptide (50 μg/ml) for 3 days. CFSE levels were measured by flow cytometry. Data are presented as the mean ± S.E.M in A and the mean ± S.D in B,D,F. *P* values were calculated using two-way ANOVA or Mann-Whitney U-test (NS, not significant; *$p < 0.05$, **$p < 0.01$, ***$p < 0.001$).

Figure 6. Bhlhe40 confers pathogenic functions of bystander $CCR6^{high}$ MP $CD4^+$ T cells by IL-1 and IL-23. (A) Predicted upstream network on IL-1β and IL-23 responded MP $CD4^+$ T cells by IPA. (B) The representative histogram and average value showing the percentage of Bhlhe40 level in $CCR6^{high}$ and $CCR6^{low}$ MP $CD4^+$ T cells induced by IL-1β/IL-23 stimulation without TCR engagement (n=3). (C) The representative percentage of IL-17A and GM-CSF expression compared to $Bhlhe40^{GFP}$ positive and negative cells in $CCR6^{high}$ MP $CD4^+$ T cells induced by IL-1β /IL-23 without TCR engagement for 5 days (n=3). (D) Representative flow cytometry plots showing the cytokine expression and (E) average proportion of WT $CCR6^{high}$ MP $CD4^+$ T cells vs. $Bhlhe40^{-/-}$ $CCR6^{high}$ MP $CD4^+$ T cells (n = 3). (F) Naïve $CD4^+$ T cells (5×10^4) from 2D2 transgenic mice were adoptively transferred, with or without WT $CCR6^{high}$ or $Bhlhe40^{-/-}$ $CCR6^{high}$ MP $CD4^+$ T cells (1×10^5, $TCR\beta^+CD1d$ $tetramer^-CD4^+CD25^-CD62L^{low}CD44^{high}$), into $Rag^{-/-}$ mice who were immunized with MOG_{35-55} in CFA. EAE clinical score was monitored daily (n=5). (G) Representative flow cytometry plots and (H) absolute cell numbers of infiltrated 2D2 TCR $(V_\beta 11^+)^-$ MP $CD4^+$ T cells (gating from $CD45^+CD4^+$) and IL-17A, GM-CSF, and IFN-γ producing cells from the spinal cords and brain on days 13 after immunization (n=5). (I) Naïve $CD4^+$ T cells (5×10^4) from 2D2 transgenic mice were adoptively transferred, with or without WT $CCR6^{high}$ or WT $CCR6^{low}$ or $GM\text{-}CSF^{-/-}$ $CCR6^{high}$ or $GM\text{-}CSF^{-/-}$ $CCR6^{low}$ MP $CD4^+$ T cells (1×10^5, $CD45.1^+TCR\beta^+CD1d$ $tetramer^-CD4^+CD25^-CD62L^{low}CD44^{high}$), into $Rag^{-/-}$ mice who were immunized with MOG_{35-55} in CFA. EAE clinical score was monitored daily (n=9). Data are presented as the mean ± S.E.M in f,i and the mean ± S.D in b,c,d,e,g,h values were calculated using two-way ANOVA or Mann-Whitney U-test (NS, not significant; *$p < 0.05$, **$p < 0.01$, ***$p < 0.001$).

Figure 1.

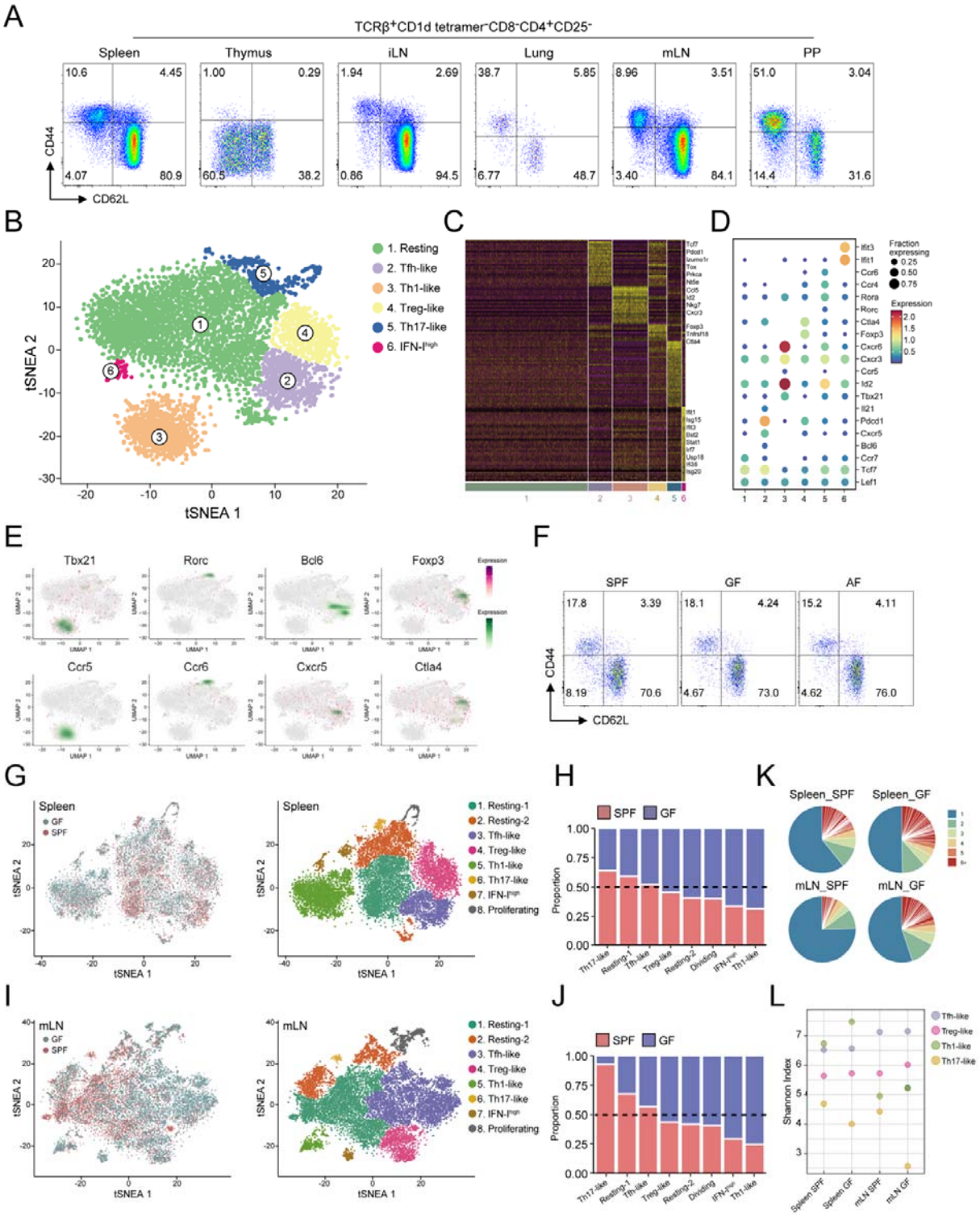

818

819

Figure 2.

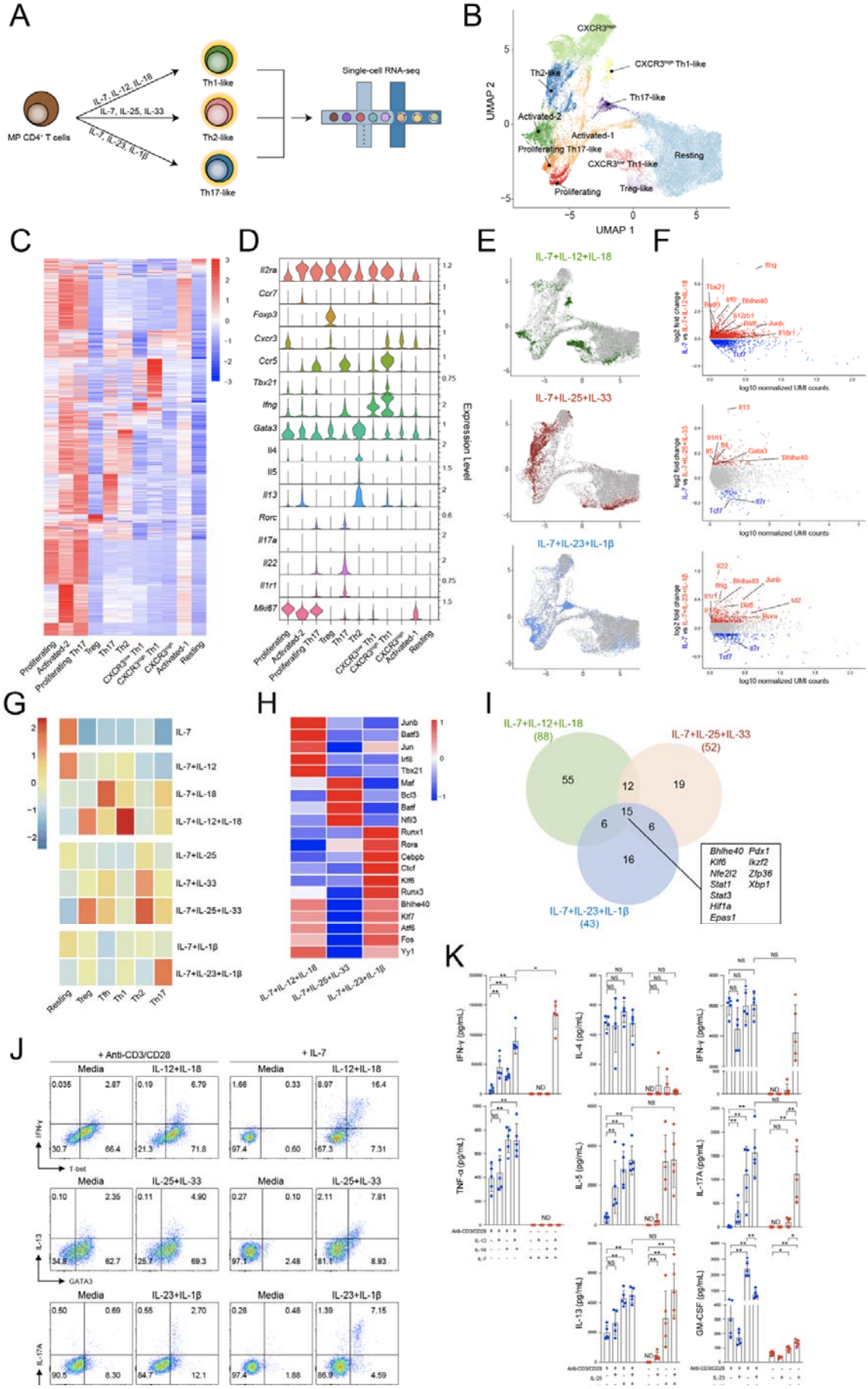
A
MP CD4+ T cells
IL-7, IL-12, IL-18
IL-7, IL-25, IL-33
IL-7, IL-23, IL-1β
Th1-like
Th2-like
Th17-like
Single-cell RNA-seq
B
UMAP 1
UMAP 2
CXCR3high
CXCR3high Th1-like
Th2-like
Th17-like
Activated-2
Activated-1
Proliferating Th17-like
CXCR3low Th1-like
Resting
Proliferating
Treg-like
C
D
Expression Level
E
IL-7+IL-12+IL-18
IL-7+IL-25+IL-33
IL-7+IL-23+IL-1β
F
log2 fold change
log10 normalized UMI counts
G
IL-7
IL-7+IL-12
IL-7+IL-18
IL-7+IL-12+IL-18
IL-7+IL-25
IL-7+IL-33
IL-7+IL-25+IL-33
IL-7+IL-1β
IL-7+IL-23+IL-1β
Resting
Treg
Th
Th1
Th2
Th17
H
I
IL-7+IL-12+IL-18 (88)
IL-7+IL-25+IL-33 (52)
IL-7+IL-23+IL-1β (43)
55
12
19
15
6
6
16
Bhlhe40 Pdx1
Klf6 Ikzf2
Nfe2l2 Zfp36
Stat1 Xbp1
Stat3
Hif1a
Epas1
J
+ Anti-CD3/CD28
+ IL-7
Media
IL-12+IL-18
IL-25+IL-33
IL-23+IL-1β
IFN-γ
T-bet
IL-13
GATA3
IL-17A
K
IFN-γ (pg/mL)
IL-4 (pg/mL)
TNF-α (pg/mL)
IL-5 (pg/mL)
IL-17A (pg/mL)
IL-13 (pg/mL)
GM-CSF (pg/mL)
ND
NS

Figure 3.

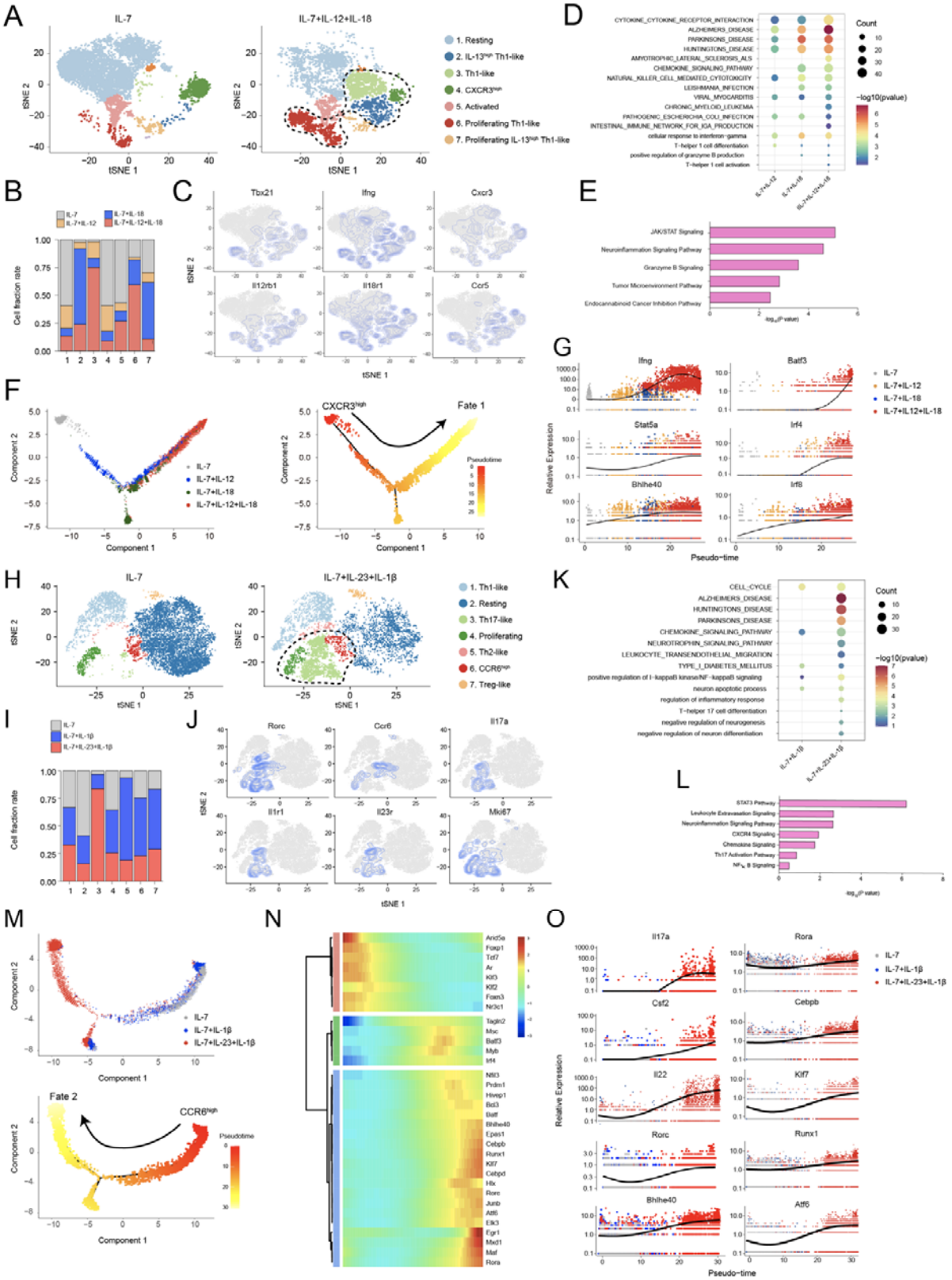
A
IL-7
IL-7+IL-12+IL-18
tSNE 1
tSNE 2
1. Resting
2. IL-13high Th1-like
3. Th1-like
4. CXCR3high
5. Activated
6. Proliferating Th1-like
7. Proliferating IL-13high Th1-like
B
Cell fraction rate
C
Tbx21
Ifng
Cxcr3
Il12rb1
Il18r1
Ccr5
D
Count
-log10(pvalue)
E
JAK/STAT Signaling
Neuroinflammation Signaling Pathway
Granzyme B Signaling
Tumor Microenvironment Pathway
Endocannabinoid Cancer Inhibition Pathway
F
Component 1
Component 2
CXCR3high
Fate 1
Pseudotime
G
Ifng
Batf3
Stat5a
Irf4
Bhlhe40
Irf8
Relative Expression
Pseudo-time
IL-7
IL-7+IL-12
IL-7+IL-18
IL-7+IL12+IL-18
H
IL-7
IL-7+IL-23+IL-1β
1. Th1-like
2. Resting
3. Th17-like
4. Proliferating
5. Th2-like
6. CCR6high
7. Treg-like
I
IL-7+IL-1β
IL-7+IL-23+IL-1β
J
Rorc
Ccr6
Il17a
Il1r1
Il23r
Mki67
K
CELL_CYCLE
ALZHEIMERS_DISEASE
HUNTINGTONS_DISEASE
PARKINSONS_DISEASE
CHEMOKINE_SIGNALING_PATHWAY
NEUROTROPHIN_SIGNALING_PATHWAY
LEUKOCYTE_TRANSENDOTHELIAL_MIGRATION
TYPE_I_DIABETES_MELLITUS
positive regulation of I-kappaB kinase/NF-kappaB signaling
neuron apoptotic process
regulation of inflammatory response
T-helper 17 cell differentiation
negative regulation of neurogenesis
negative regulation of neuron differentiation
L
STAT3 Pathway
Leukocyte Extravasation Signaling
Neuroinflammation Signaling Pathway
CXCR4 Signaling
Chemokine Signaling
Th17 Activation Pathway
NFκ B Signaling
M
Fate 2
CCR6high
N
O
Il17a
Rora
Csf2
Cebpb
Il22
Klf7
Rorc
Runx1
Bhlhe40
Atf6
IL-7+IL-1β
IL-7+IL-23+IL-1β

Figure 4.

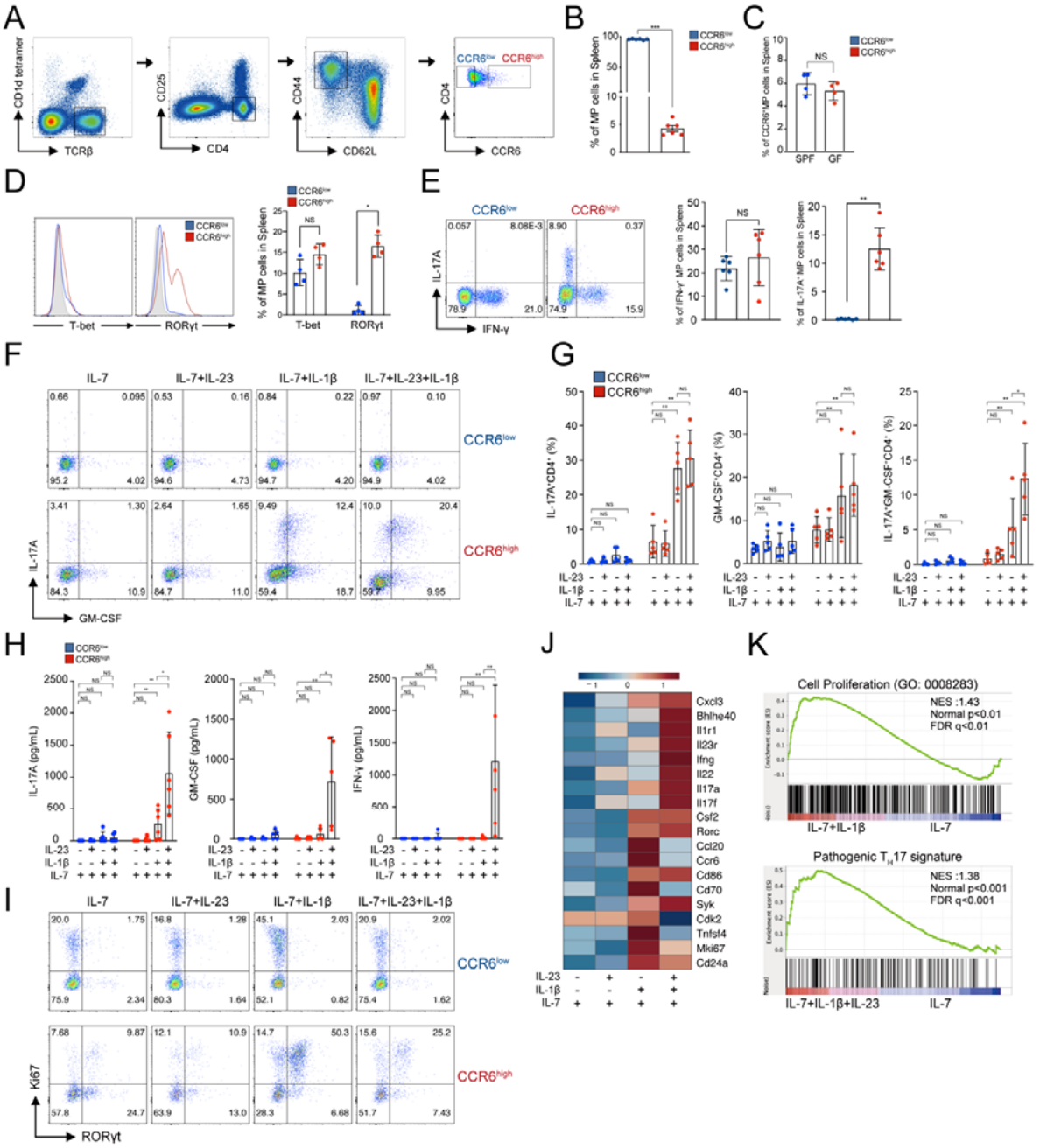
A
CD1d tetramer
TCRβ
CD25
CD4
CD44
CD62L
CD4
CCR6
CCR6low
CCR6high
B
% of MP cells in Spleen
C
% of CCR6high MP cells in Spleen
SPF
GF
NS
D
T-bet
RORγt
% of MP cells in Spleen
E
IL-17A
IFN-γ
% of IFN-γ+ MP cells in Spleen
% of IL-17A+ MP cells in Spleen
F
IL-7
IL-7+IL-23
IL-7+IL-1β
IL-7+IL-23+IL-1β
GM-CSF
G
IL-17A+CD4+ (%)
GM-CSF+CD4+ (%)
IL-17A+GM-CSF+CD4+ (%)
IL-23
IL-1β
IL-7
H
IL-17A (pg/mL)
GM-CSF (pg/mL)
IFN-γ (pg/mL)
I
Ki67
RORγt
J
Cxcl3
Bhlhe40
Il1r1
Il23r
Ifng
Il22
Il17a
Il17f
Csf2
Rorc
Ccl20
Ccr6
Cd86
Cd70
Syk
Cdk2
Tnfsf4
Mki67
Cd24a
K
Cell Proliferation (GO: 0008283)
NES :1.43
Normal p<0.01
FDR q<0.01
IL-7+IL-1β
IL-7
Pathogenic TH17 signature
NES :1.38
Normal p<0.001
FDR q<0.001
IL-7+IL-1β+IL-23
IL-7

Figure 5.

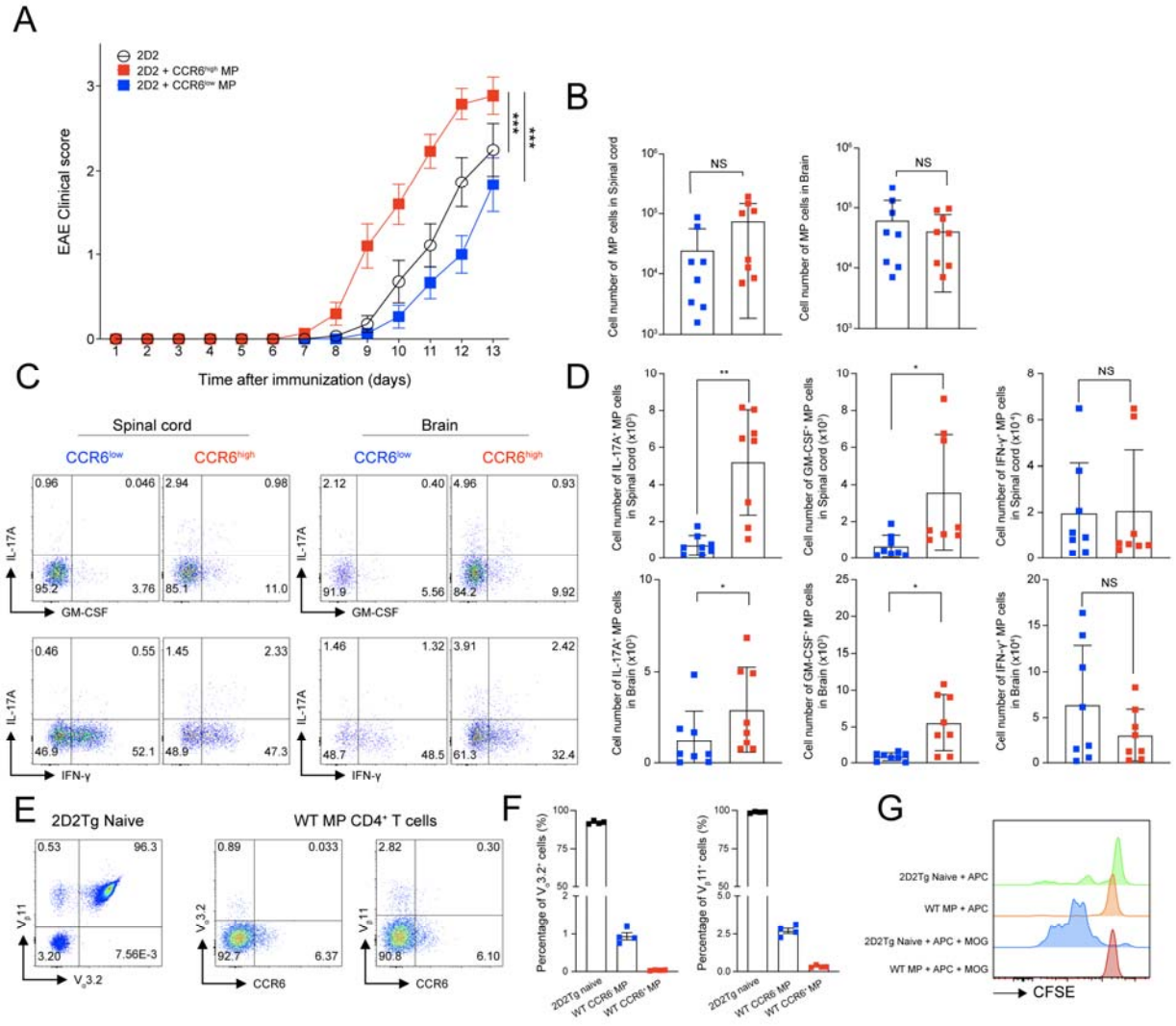
A
2D2
2D2 + CCR6high MP
2D2 + CCR6low MP
EAE Clinical score
Time after immunization (days)
***
***
B
Cell number of MP cells in Spinal cord
Cell number of MP cells in Brain
NS
NS
C
Spinal cord
Brain
CCR6low
CCR6high
CCR6low
CCR6high
IL-17A
GM-CSF
IFN-γ
D
Cell number of IL-17A+ MP cells in Spinal cord (x10³)
Cell number of GM-CSF+ MP cells in Spinal cord (x10³)
Cell number of IFN-γ+ MP cells in Spinal cord (x10³)
Cell number of IL-17A+ MP cells in Brain (x10³)
Cell number of GM-CSF+ MP cells in Brain (x10³)
Cell number of IFN-γ+ MP cells in Brain (x10³)
NS
E
2D2Tg Naive
WT MP CD4+ T cells
Vα3.2
Vβ11
CCR6
F
Percentage of Vα3.2+ cells (%)
Percentage of Vβ11+ cells (%)
2D2Tg naive
WT CCR6 MP
WT CCR6- MP
G
2D2Tg Naive + APC
WT MP + APC
2D2Tg Naive + APC + MOG
WT MP + APC + MOG
CFSE

Figure 6.

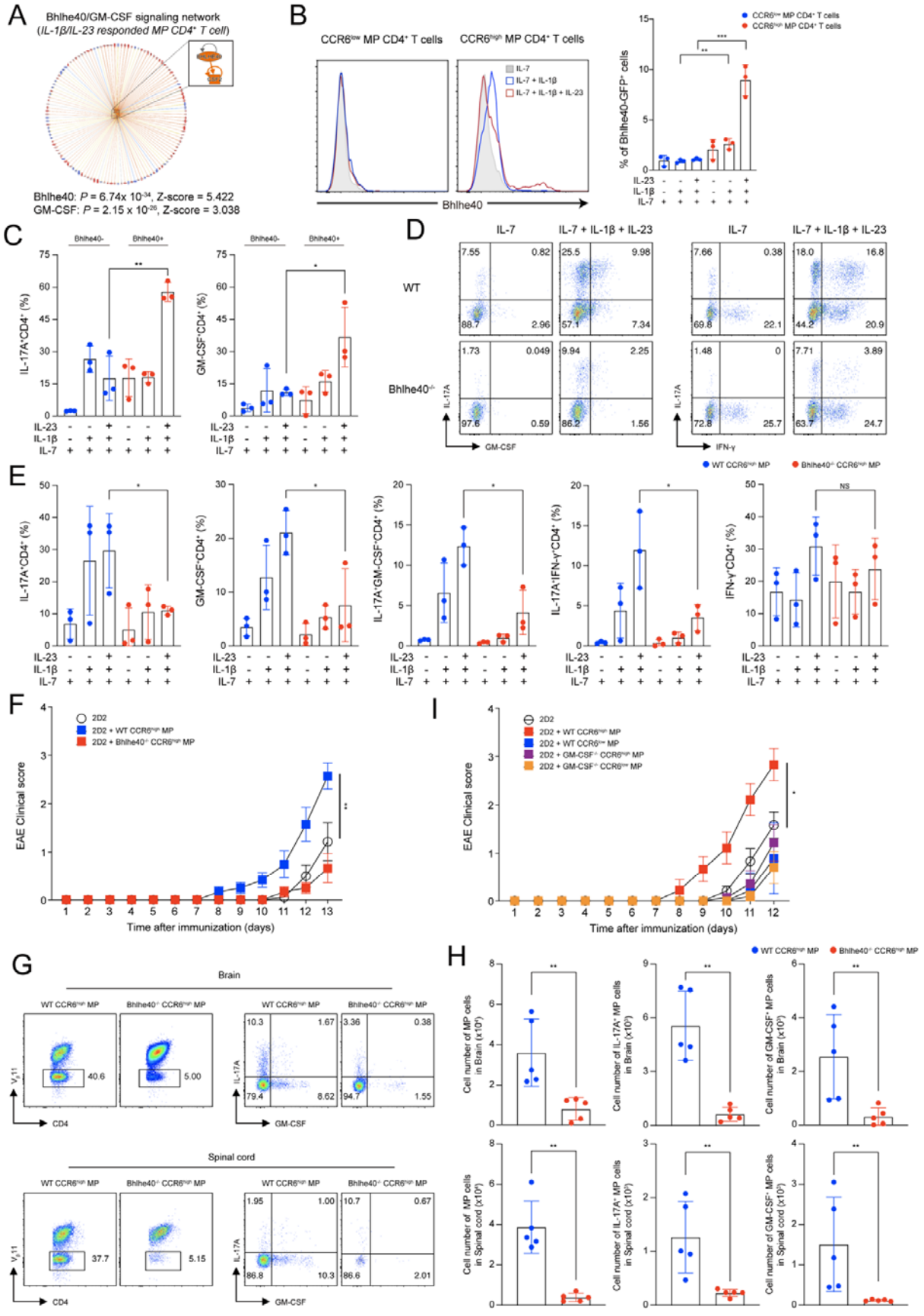
A
Bhlhe40/GM-CSF signaling network
(IL-1β/IL-23 responded MP CD4+ T cell)
Bhlhe40: P = 6.74x 10-34, Z-score = 5.422
GM-CSF: P = 2.15 x 10-26, Z-score = 3.038
B
CCR6low MP CD4+ T cells
CCR6high MP CD4+ T cells
IL-7
IL-7 + IL-1β
IL-7 + IL-1β + IL-23
Bhlhe40
% of Bhlhe40-GFP+ cells
C
Bhlhe40-
Bhlhe40+
IL-17A+CD4+ (%)
GM-CSF+CD4+ (%)
IL-23
IL-1β
IL-7
D
IL-7
IL-7 + IL-1β + IL-23
WT
Bhlhe40-/-
IL-17A
GM-CSF
IFN-γ
WT CCR6high MP
Bhlhe40-/- CCR6high MP
E
IL-17A+CD4+ (%)
GM-CSF+CD4+ (%)
IL-17A+GM-CSF+CD4+ (%)
IL-17A+IFN-γ+CD4+ (%)
IFN-γ+CD4+ (%)
NS
F
2D2
2D2 + WT CCR6high MP
2D2 + Bhlhe40-/- CCR6high MP
EAE Clinical score
Time after immunization (days)
I
2D2
2D2 + WT CCR6high MP
2D2 + WT CCR6low MP
2D2 + GM-CSF-/- CCR6high MP
2D2 + GM-CSF-/- CCR6low MP
EAE Clinical score
Time after immunization (days)
G
Brain
WT CCR6high MP
Bhlhe40-/- CCR6high MP
Vγ11
CD4
IL-17A
GM-CSF
Spinal cord
H
WT CCR6high MP
Bhlhe40-/- CCR6high MP
Cell number of MP cells in Brain (x10³)
Cell number of IL-17A+ MP cells in Brain (x10³)
Cell number of GM-CSF+ MP cells in Brain (x10³)
Cell number of MP cells in Spinal cord (x10³)
Cell number of IL-17A+ MP cells in Spinal cord (x10³)
Cell number of GM-CSF+ MP cells in Spinal cord (x10³)

Supporting Information

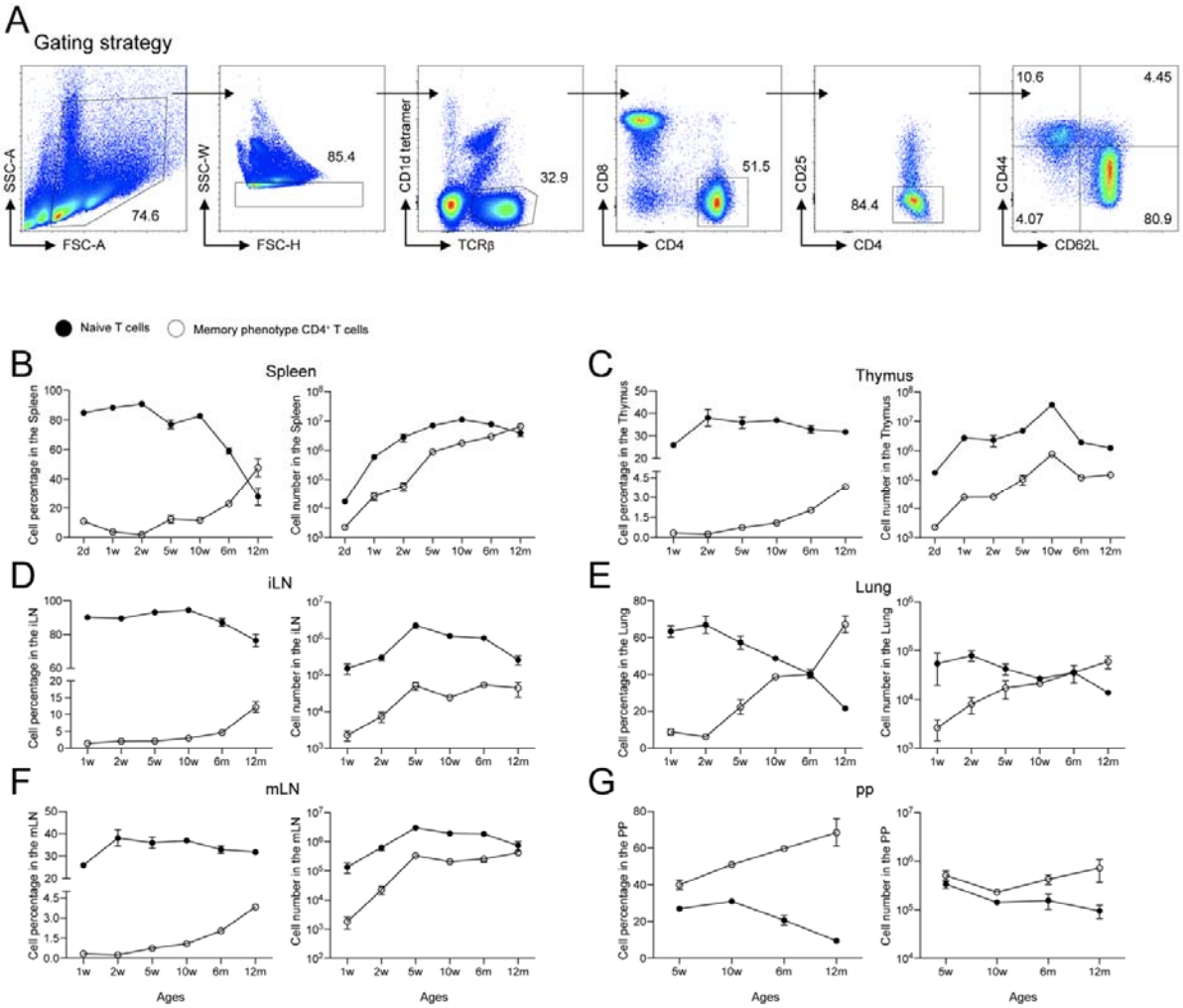

Figure S1. CD44^{high} memory phenotype (MP) CD4^{+} T cells increase with age in mice. (A) Gating strategy of Splenic MP CD4^{+} T cells (TCRβ^{+}CD1d tetramer^{-}CD8^{-}CD4^{+}CD25^{-}CD62L^{low}CD44^{high}). Analysis of cell percentage and number of naïve (TCRβ^{+}CD1d tetramer^{-}CD8^{-}CD4^{+}CD25^{-}CD62L^{high}CD44^{low}) and MP CD4^{+} T cells (TCRβ^{+}CD1d tetramer^{-}CD8^{-}CD4^{+}CD25^{-}CD62L^{low}CD44^{high}) by age from (B) the spleen, (C) thymus, (D) iLN, (E) lung, (F) mLN, and (G) PP.

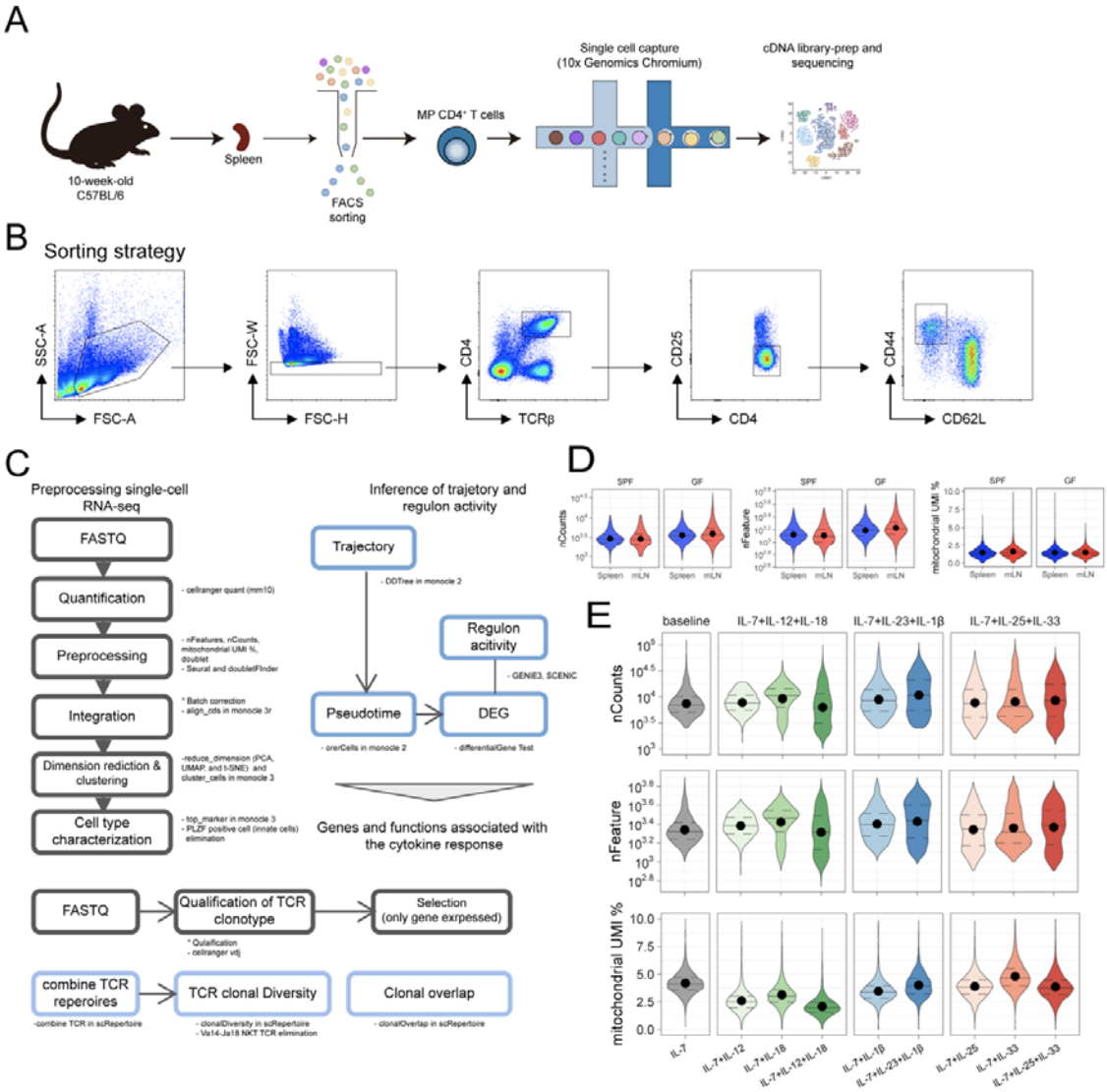

Figure S2. Strategy and flow of single cell RNA-sequencing analysis. (A) Visual concept of scRNA-seq for MP $CD4^+$ T cells. (B) Gating strategy of splenic MP ($TCR\beta^+CD4^+CD25^-CD62L^{low}CD44^{high}$) $CD4^+$ T cells. (C) Workflow of scRNA-seq and TCR-seq of PLZF and TCR $V_\alpha14$-$J_\alpha18$ (TRAV11-TRAJ18) negative MP $CD4^+$ T cells. (D) Quality measures of splenic and mLN MP $CD4^+$ T cells from SPF- and GF–housed mice. (E) QC metrics for each condition of MP $CD4^+$ T cells. (nFeature: the number of expressed genes per cell, nCounts: the number of total UMI counts per cell, mitochondrial UMI %: the percentage of UMI counts of mitochondrial genes per cell)

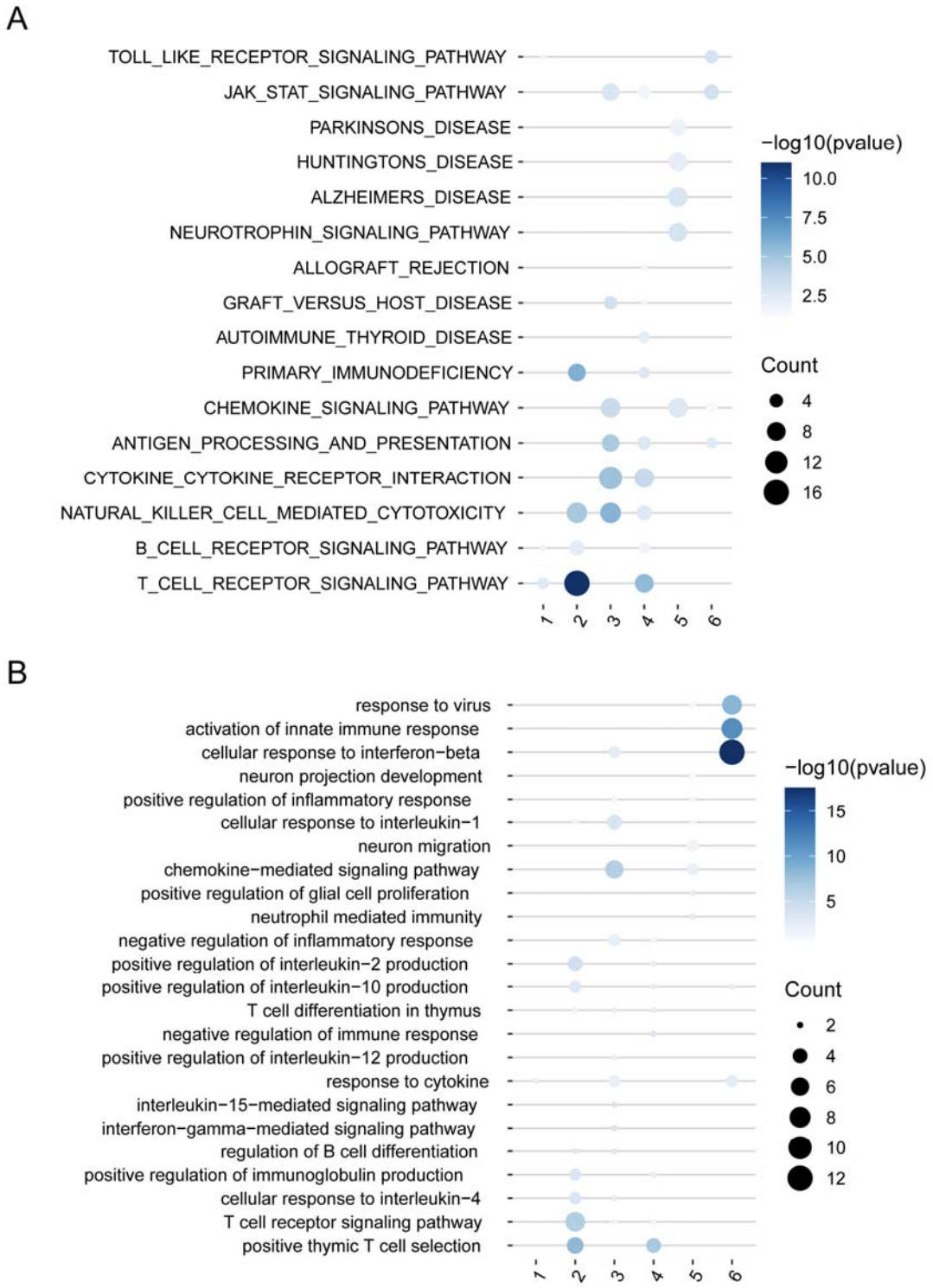

Figure S3. KEGG/GO analysis of steady-state MP CD4$^+$ T cells. Selected (A) KEGG and (B) GO terms in each subpopulation of splenic MP CD4$^+$ T cells.

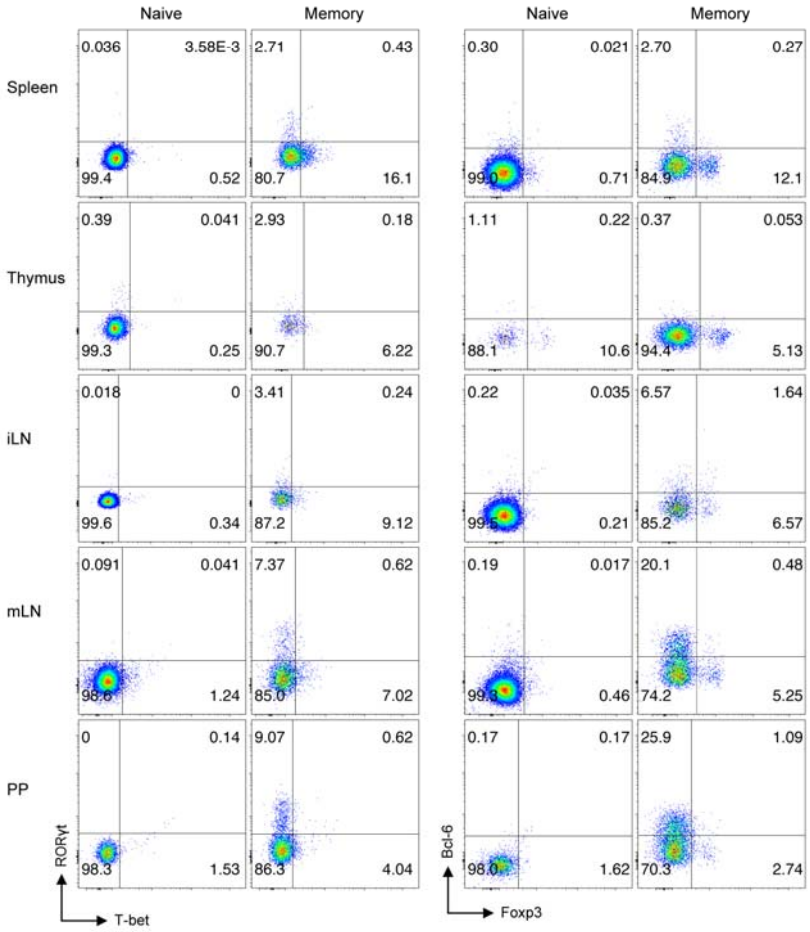

Figure S4. Effector T cell lineage–specific marker expression in MP CD4$^+$ T cells. Transcription factor expression levels of T-bet, RORγt, Bcl-6, and Foxp3 in naïve and MP CD4$^+$ T cells from the spleen, thymus, iLN, mLN, and PP.

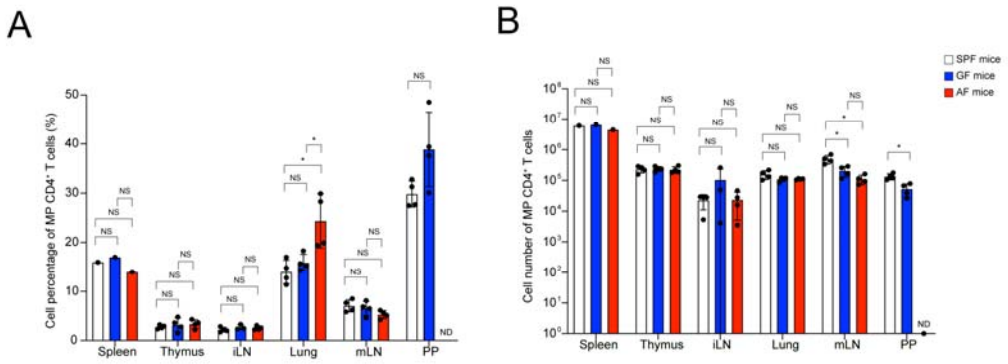

Figure S5. Comparison of MP CD4^{+} T cells in tissues from SPF, GF, and AF mice. (A) Proportion and (B) number of MP CD4^{+} T cells in the spleen, thymus, iLN, lung, mLN, and PP in SPF, GF, and AF mice (n=4). Data are presented as the mean ± S.D. P values were calculated using Mann-Whitney U-test (ND, not detected; NS, not significant; *$p < 0.05$, **$p < 0.01$, ***$p < 0.001$).

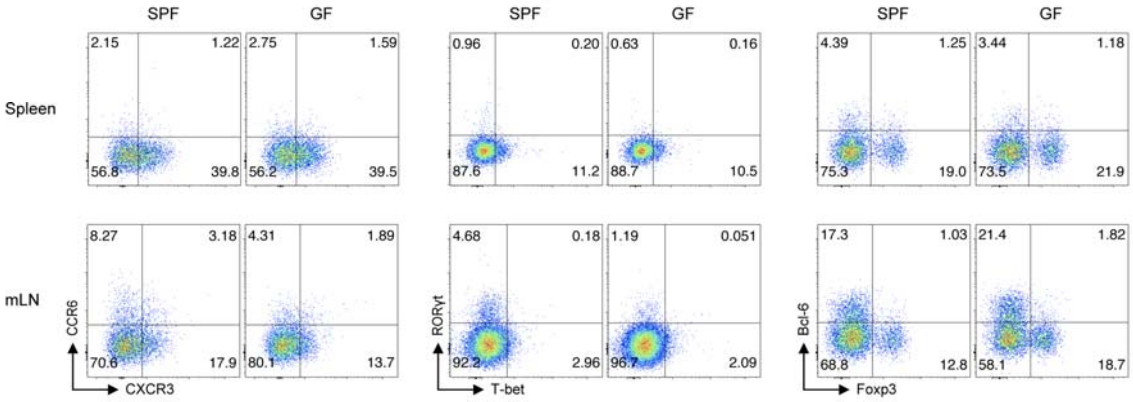

Figure S6. Effector T cell lineage–specific chemokine receptors and transcription factors in MP CD4$^+$ T cells from SPF and GF mice. Expression of chemokine receptor of CCR6, CXCR3 and transcription factors of T-bet, RORγt, Bcl-6, and Foxp3 in spleen- and mLN-derived MP CD4$^+$ T cells from SPF and GF mice.

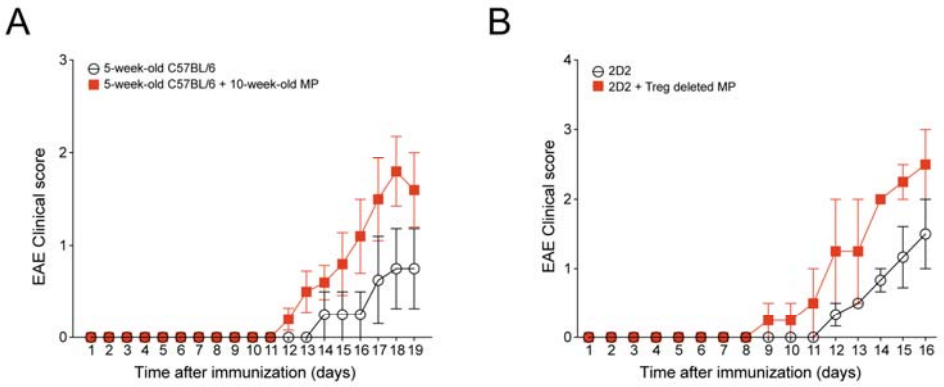

Figure S7. MP CD4^{+} T cells exacerbate autoimmune encephalomyelitis. (A) 5-week-old C57BL/6 mice with or without adoptively transferred 5 × 10^{5} MP CD4^{+} T cells (TCRβ^{+}CD1d tetramer^{-}CD4^{+}Foxp3^{-}CD62L^{low}CD44^{high}) from 10-week-old Foxp3-GFP mice were induced EAE by MOG_{35-55} in CFA (n=4). (B) 5 × 10^{4} naïve CD4^{+} T cells (TCRβ^{+}CD4^{+}V_{β}11^{+}CD25^{-}CD62L^{high}CD44^{low}) from 2D2 transgenic mice were adoptively transferred, with or without 5 ×10^{5} splenic Treg-deleted MP CD4^{+} T cells (TCRβ^{+}CD1d tetramer^{-}CD4^{+}Foxp3^{-}CD62L^{low}CD44^{high}) sorted from Foxp3-GFP mice, into Rag$^{-/-}$ mice who were immunized with MOG_{35-55} in CFA (n = 3).